FUNCTIONALIZED PHOTOSENSITIVE POLYMERIC NANOCARRIERS FOR SPECIFIC DELIVERY OF CARGO IN CARDIOMYOCYTES

PEDRO ALEJANDRO MENA GIRALDO

UNIVERSIDAD PONTIFICIA BOLIVARIANA

ENGINEERING SCHOOL

MASTER IN ENGINEERING

MEDELLÍN-COLOMBIA

2017

FUNCTIONALIZED PHOTOSENSITIVE POLYMERIC NANOCARRIERS FOR SPECIFIC DELIVERY OF CARGO IN CARDIOMYOCYTES

PEDRO ALEJANDRO MENA GIRALDO

Master's thesis to obtain the degree Magister in Engineering

Biomedical Engineering area

Director:

PhD. Lina Hoyos Palacio

Chemical Engineer

Adviser:

PhD. Jahir Orozco Holguín

Chemist

Adviser:

MSc. Sandra Pérez Buitrago

Bioengineer

UNIVERSIDAD PONTIFICIA BOLIVARIANA

ENGINEERING SCHOOL

MASTER IN ENGINEERING

MEDELLÍN-COLOMBIA

2017

Pedro Alejandro Mena Giraldo

"I declare that this master´s thesis has not been submitted to qualify for a degree, either in the same way or with variations, in this or any other university" Art 82 “Régimen Discente” of advanced formation.

Sign

Acknowledgments

I give my sincere acknowledgment to:

COLCIENCIAS for the financial support to the project entitled: "*DESARROLLO DE NANOSISTEMAS PARA LA DISTRIBUCIÓN ACTIVA DE FOTOSENSIBILIZADORES EN CÉLULAS CARDIACAS* - radicado 369B-03/15-04", from Universidad Pontificia Bolivariana.

MSc. Sandra Pérez (from Universidad Pontificia Bolivariana) for her high contribution in the development of the project as an adviser and co-researcher of project from COLCIENCIAS.

PhD. Jahir Orozco (from the Max Planck Tandem Group in Nanobioengineering, Universidad de Antioquia) for his direction, accompaniment and advice in the development of the master thesis as co-tutor and for the functionalization and characterization processes.

PhD. Lina Hoyos (from the Molecular Biology group, Universidad Pontificia Bolivariana) for her direction, accompaniment and advice in the master thesis as a tutor.

PhD. Isabel Ortiz (from the Molecular Biology group, Universidad Pontificia Bolivariana) for training in the process of cell culture and maintenance of the cardiac cells.

PhD. Diana Alzate from UANL and PhD. Alejandra Garcia from CIMAV for their collaboration in the nanocarriers characterization process.

PhD. Carolina Camargo (from Max Planck Tandem Group in Mosquito Reproductive Biology) for her help with edition of the manuscript.

Contents

Lists of abbreviations

AF	Atrial fibrillation
PNcs	Photosensitive Nanocarriers
CTC	Cardiac Targeting Peptide
FITC	Fluorescein Isothiocyanate
FITC-CTC	FITC-Modified Cardiac Targeting Peptide
NBc	Nanobioconjugate
UV	Ultra Violet
PBS	Phosphate Buffer Saline
EDC	1-Ethyl-3-(3-dimethylaminopropyl) carbodiimide
NHS	N-hydroxysuccinimide
HEPES	2-[4-(2-hydroxyethyl)piperazin-1-yl]ethanesulfonic acid
DLS	Dispersion Light Scattering
SEM	Scanning Electron Microscopy
TEM	Transmission Electron Microscopy
MTT	3-(4,5-dimethylthiazol-2-yl)-2,5-diphenyltetrazolium bromide

Abstract

This investigation is in the frame of the project entitled "*Desarrollo de nanosistemas para la distribución activa de fotosensivilizadores en células cardiacas*" financed by COLCIENCIAS and executed by the Cardiovascular Dynamics and Systems Biology research groups both of them from Universidad Pontificial Bolivariana.

To reduce side effects of the currents treatments (pharmacologic and cardiac ablation) for the cardiovascular disease atrial fibrillation (AF), and increase the therapeutic efficiency of pharmacological treatments, this master thesis proposes a functional photoresponsive polymeric nanocarrier for intracellular drug delivery in cardiac cells (cardiomyocytes), as an alternative treatment for AF. Thus, a Nanobioconjugate (NBc) with specific affinity to cardiomyocytes was developed by means of functionalization of the photosensitive nanocarriers (PNcs) with the transmembrane peptide (Cardiac Targeting Peptide - CTP) as bioreceptor.

The bioreceptor was coupled to the nanocarriers by covalent linking using 1-Ethyl-3-(3-dimethylaminopropyl) carbodiimide (EDC) and N-hydroxysuccinimide (NHS) as catalyzers. The resultant NBc was characterized in terms of morphology, particle size and charge and functionalization extent by imaging techniques such as Scanning Electron Microscopy (SEM) and Transmission Electron Microscopy (TEM), Dynamic Light Scattering (DLS), z potential and ultraviolet–visible (UV-vis) spectroscopy.

Affinity of the NBc for the cardiomyocytes was demonstrated by fluorescence microscopy experiments, which showed that the NBc were internalized in the cellular cytoplasm through the endocytosis mechanism. The NBc occupy 15.90 % average of the cardiomyocytes area (after 8 h of incubation), when using a concentration of 0.150 mg/ml of NBc. Such NBc concentration resulted to be biocompatible as demonstrated by 3-(4,5-dimethylthiazol-2-yl)-2,5-diphenyltetrazolium bromide (MTT) viability experiments.

Resumen

Esta investigación está enmarcada dentro del proyecto titulado "*Desarrollo de nanosistemas para la distribución activa de fotosensibilizadores en células cardiacas*", el cual fue financiado por COLCIENCIAS y ejecutado por los grupos de investigación en Dinámica Cardiovascular y en Biología de Sistemas de la Universidad Pontificia Bolivariana.

Para reducir los efectos secundarios de los tratamientos actuales (farmacológicos y ablación cardiaca) de la fibrilación auricular (enfermedad cardiovascular) y aumentar la eficiencia terapéutica de los tratamientos farmacológicos, en este trabajo de maestría, se propone un nano-transportador polimérico fotosensible funcional, con la capacidad de liberar medicamentos de manera intracelular en cardiomiocitos (células cardiacas), como tratamiento alternativo para la fibrilación auricular. En este contexto, se desarrolló un nanobioconjugado con afinidad específica por cardiomiocitos, mediante la funcionalización de los nano-transportadores fotosensibles con un péptido transmembrana (bioreceptor).

El bioreceptor fue conjugado con los nano-transportadores mediante reacción covalente usando EDC y NHS como catalizadores. El NBc resultante, se caracterizó en términos de la morfología, tamaño de partícula, carga y grado de funcionalización, mediante SEM y TEM, DLS, potencial z y UV-vis.

La afinidad del nanobioconjugado por los cardiomiocitos se demostró mediante microscopia de fluorescencia, cuyas imágenes mostraron que los NBc se internalizan en el citoplasma celular, a través del mecanismo de endocitosis. Estos ocupan en promedio el 15.90 % del área celular (después de 8 horas de incubación), con una concentración de 0.150 mg/ml del NBc, que demostró ser biocompatible, mediante la técnica de viabilidad con MTT.

CHAPTER I:

INTRODUCTION, PROBLEM STATEMENT, HYPOTHESIS AND OBJECTIVES

1.1 Introduction and Problem Statement

Atrial fibrillation (AF), is the most common sustained arrhythmia associated with substantial cardiovascular morbidity and mortality with stroke being the most critical complication [1]. In Latin America, AF is estimated to be responsible for approximately 15–20% of all strokes, and patients with AF have a 3–4% risk per year of developing stroke [2]. Atrial Fibrillation (AF) affects between 1% and 2% of general population, with a peak prevalence of 10% in those older than 80 years. It is estimated that by 2050 nearly 16 million US patients will have AF [3].

Its prevalence increases with age as areas of fibrosis and scars may be developed on the atrial walls. AF exacerbates the prognosis of patients with acute myocardial infarction and hospitalized patients with heart failure. Moreover, AF can double the mortality rate, independently of other known cardiovascular conditions [4]. For all of the above, AF is a disease that generates significant expenses in health systems [5].

Chronic AF includes either episodes that exceed seven days, which may continue for more than one year (Persistent AF), or constant episodes in which it is not possible returning to sinus rhythm by medication or cardioversion (Permanent AF) [6]. Under these conditions, chronic AF treatment consists of drug control and catheter ablation. In pharmacological therapy, collateral effects have been observed to increase the patient risk such as bradycardia, thyroid and renal dysfunction, as well as proarrhythmic effects. In ablation, regardless of the energy used, whether radiofrequency (RF), cryoenergy, laser or ultrasound, there is a handicap due to the non-specific nature of the resulting cell damage. In this context, ablation can lead to complications such as atrioesophageal fistula, stenosis of the pulmonary veins, or coronary artery injury. In addition, lack of cellular discrimination increases the energy required for ablation and may prolong procedure times [4] [7].

Some researchers have pointed out the urgent necessity of circumvent the aforementioned limitations with novel, less adverse and effective methods for delivering atrial-specific pharmacological agents to treat AF. For example, Avula (2012) and co-workers claimed the imperative requirement of targeted photoresponsive nanoparticles, for this purpose: "*Finally, a similar approach may also help deliver antiarrhythmic drugs in a cell-specific manner. As an example, ventricular proarrhythmic effects of common antiarrhythmic drugs represent a major limitation of atrial fibrillation management and atrial-specific*

pharmacological agents are highly desirable. Targeted biodegradable nanoparticles that release drugs upon illumination may be implemented to release an antiarrhythmic drug only to atrial myocytes. Such highly selective drug administration would drastically reduce the global dose, and thus any potential side effects" [8]. The Group of Research in Cardiovascular Dynamic from the Universidad Pontificia Bolivariana has developed a photosensitive nanocarriers (PNcs) to achieve temporal specificity in drug delivery. The PNcs were developed based on chitosan biopolymer, photoactivatable by ultra violet (UV) light of long wavelength [9], through the design of a new methodology to synthesize the novel amphiphilic photoresponsive biopolymer. The nanoparticles were formed by the nanoprecipitation method, in order to get nanomicells with the azobenzene group as photosensitive molecule in the hydrophobic center and a carboxylic group in the hydrophilic external surface, as depicted in Figure 1. With this design, the NPs can transport both hydrophobic drugs and photosensitizers in aqueous medium, such as blood (see Figure 2).

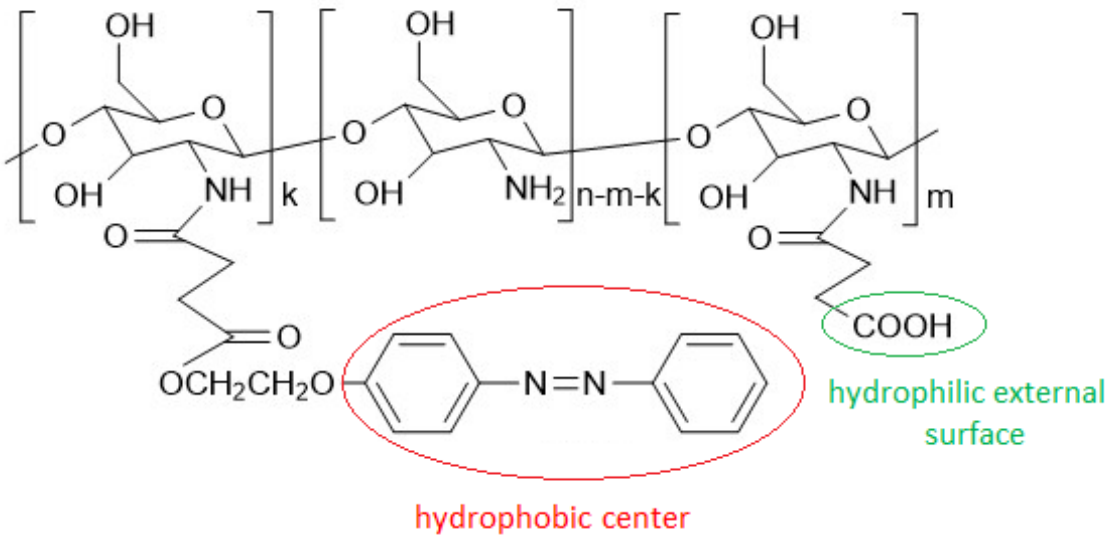

Figure 1. Precursor molecule for the Photosensitive Nanocarriers (PNcs). Where, the polymeric units, n corresponds to chitosan, k is the chitosan functionalized with the photosensitive molecule (4-phenylazophenol) and m is N-succinyl chitosan, thus n-m-k is the polymeric unit n united to k and m.

Development of temporal and spatial treatments are necessary to reduce side effects from pharmacological therapy and discrimination of energy in the ablation process. The PNcs with temporal specificity has been already developed by the Cardiovascular Dynamic Research Group as described above. However, this molecule lacks of spatial specificity, necessary for the nanoparticles interact directly with the cardiac cells (cardiomyocytes) to

fight the AF. Based on the need of obtaining a specific therapy to potentiate the therapeutic effect of temporal and spatial treatments, the research question of this study was:

How to direct photosensitive nanocarriers specifically to cardiomyocytes?

The need of making triggered delivery of drugs in cardiac cells as atrial fibrillation treatment was first expressed by Avula, as commented above "*to release an antiarrhythmic drug only to atrial myocytes"* and recently pointed out again by Ravens et al. (2017) *"atrial-selective release of* drug" as shown as following "*Ideally, drugs should only affect atrial targets without any influence on the ventricles. For instance, excessive prolongation in ventricular APD by conventional class III antiarrhythmic drugs (mainly hERG channel blockers) is associated with a high risk of life-threatening torsades de pointes arrhythmias that may exacerbate into ventricular fibrillation. To circumvent this problem the concept of "atrial-selective" drug development has attracted enormous scientific and pharmaceutical interest in identifying novel targets for drugs to treat atrial fibrillation"* [10].

Specific intracellular release of drugs into cardiac cells can be achieved through a bioreceptor, with affinity to cardiomyocytes, functionalized on the surface of the photosensitive nanocarriers. Thus, a possible therapy to treat the AF by phototriggered drug delivery with temporal and spatial specificity is presented herein as depicted in Figure 2.

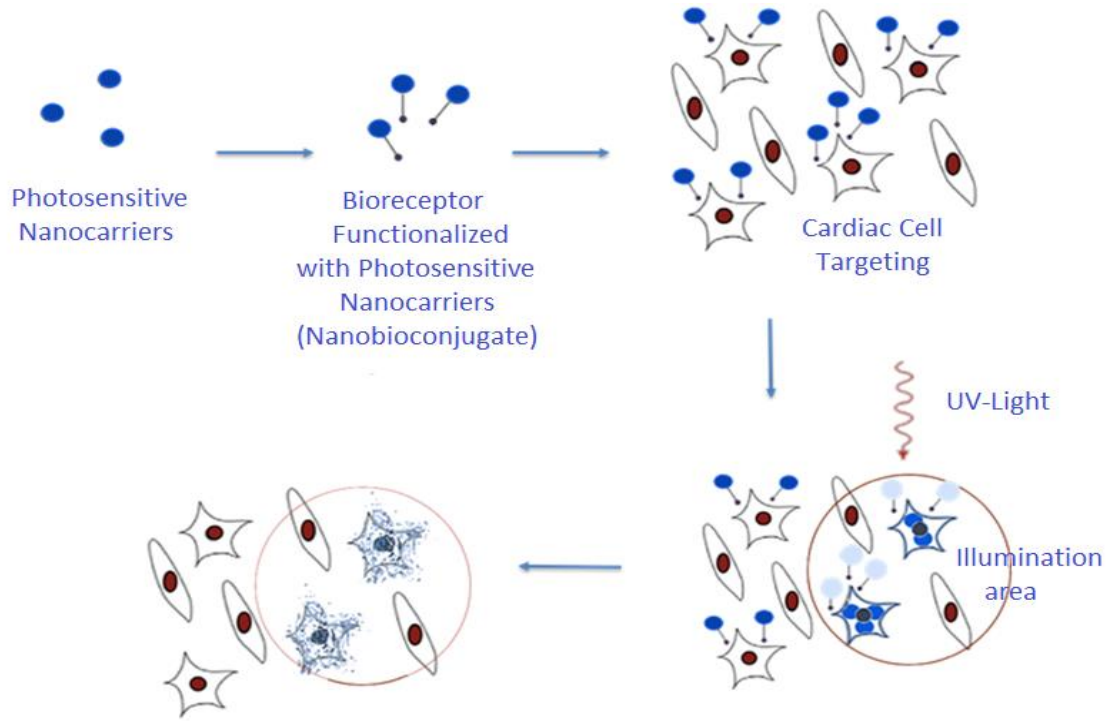

Figure 2. Sketch of the concept: functional photosensitive nanocarriers for specific drug delivery in cardiac cells.

1.2 Hypothesis

A peptide bioreceptor linked to the surface of UV-photosensitive nanocarriers (nanobioconjugates) promote both, their selective adhesion and more effective internalization by cardiomyocyte cells for further localized phototriggered drug delivery.

Objectives

General Objective

- To functionalize photosensitive polymeric nanocarriers with a bioreceptor for the selective release of drugs in cardiomyocytes.

Specific Objectives

- To select a specific bioreceptor with affinity to cardiomyocytes.
- To design and implement the chemical process for the functionalization of the photosensitive polymeric nanocarriers with the specific bioreceptor (development of nanobioconjugates).
- To characterize the photosensitive nanocarriers functionalized with the specific bioreceptor in terms of morphology, particle size, charge and concentration.
- To evaluate the specificity of the nanobioconjugates for the cardiomyocyte cells.

CHAPTER II:

FRAMEWORK AND STATE OF THE ART

2.1 Framework

Nanocarriers system of active principles

Nanocarriers are systems composed of different biodegradable materials such as natural polymers, lipids, phospholipids, among others. Their size is commonly between 100 and 1000 nm [11]. For this reason, they can be compared with natural or biological nanocarriers such as proteins, DNA, and viruses, which are in the order of few tens of nm; and with cells and cell assemblies that are in the order of the few µm in size. Synthetic nanocarriers comprise a wide range of systems, such as: nanotubes, liposomes, solid lipid nanoparticles, polymeric nanoparticles, polymeric micelles, dendrimers and functionalized nanoparticles [12]. They can be tailored designed for transporting a variety of active principles, either encapsulated, adsorbed or dispersed. Their small size commonly allows for crossing physiological barriers in the body. Their intrinsic properties may account not only for improving the solubility of poorly soluble drugs in water and increasing the residence time in the body, but also for reducing the toxicity and adverse effects of some medications and controlling the space- and time-specific release of active principles in, among others. However, these systems suffer from some limitations such as storage stability and the type of administration, as they are susceptible to aggregation and early degradation processes. They may also access unwanted sites and generate genetic damage and/or mutations. In this context, there is an obvious need to develop functional nanocarrier systems to encapsulate drugs, allowing for their further controlled and efficient site-specific targeted delivery [11].

The systems most used in the encapsulation of hydrophobic drugs are generally composed by a hydrophobic segment, that allows interaction with the drug and a hydrophilic segment that gives stability to the nanocarriers and improve their interaction with the physiological environment. Within these systems, polymeric nanoparticles (nanospheres and nanocapsules), liposomes and polymeric micelles are the most frequently options (Figure 3) [13] [14].

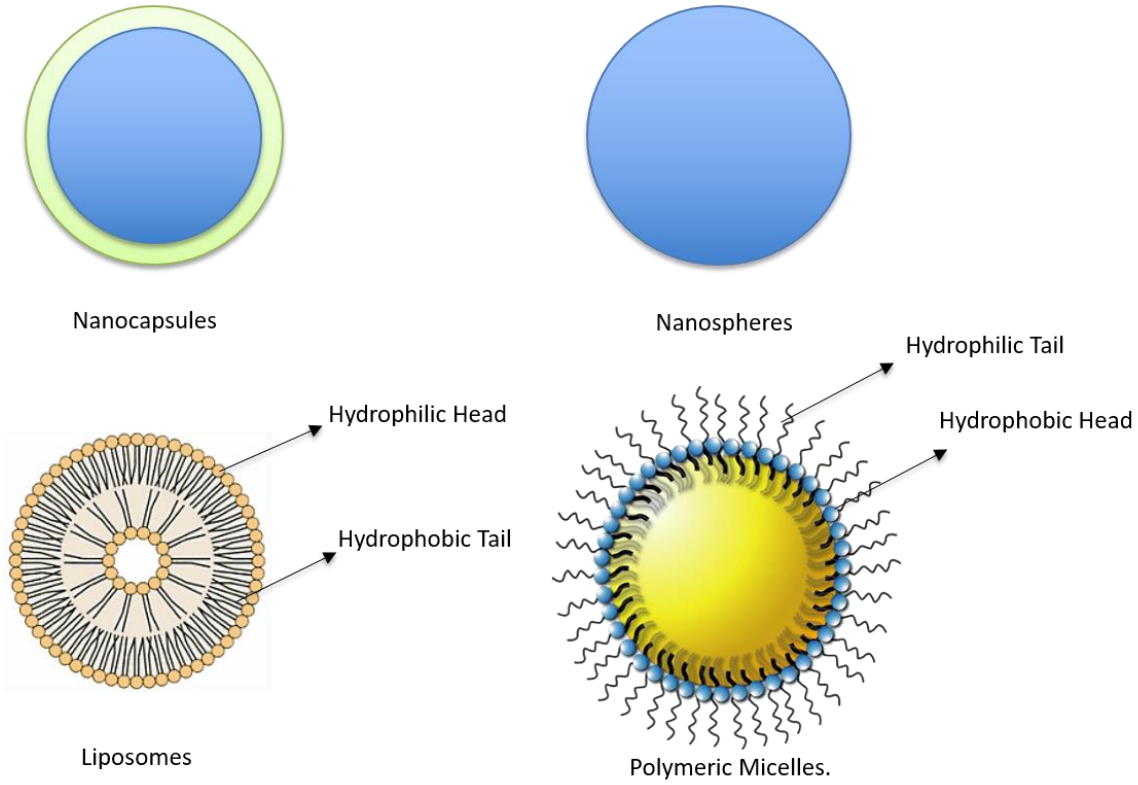

Figure 3. Nanocarriers with capacity to transport hydrophobic active principles [13] [14].

Polymeric Nanomicelles

Polymeric nanomicelles systems include amphiphilic block copolymers and surfactants that self-assemble in aqueous solutions and form micellar systems of colloidal size. The hydrophobic blocks of the amphiphilic polymer move away from this aqueous medium to reach the minimum free energy state. This energy increases due to unfavorable interactions between the water molecules and the hydrophobic region of the amphiphilic polymer. The critical micellar concentration (CMC) is a specific concentration of amphiphilic polymer, above which, the micelles are thermodynamically stable. In contrast, if the concentration of the amphiphilic polymer is below of the CMC, the micelles tend to disassemble [15] [16]. As the nanomicelles have a core-shell type structure, with a hydrophobic center and hydrophilic surface; they have the ability to transport hydrophobic drugs inside the core-shell, keeping their stability when displacing in aqueous medium (Figure 4).

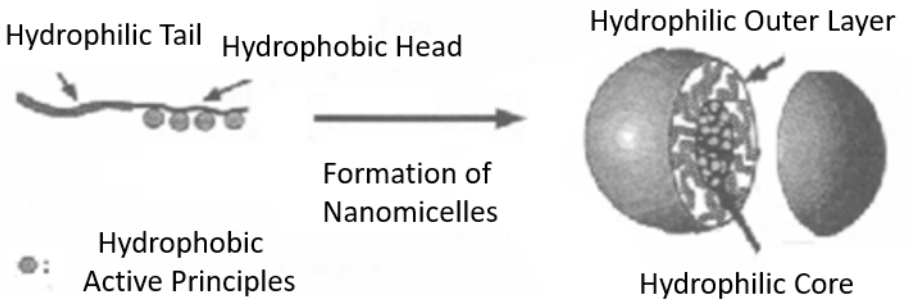

Figure 4. Structure of the nanomicelles in the process of encapsulating a hydrophobic active principle. Reproduced from [17].

2.2 State of the art

Atrial Fibrillation

Atrial fibrillation (AF) is the most common cardiac arrhythmia in humans. It is associated with increased morbidity and mortality and it has become a first order public health problem. In AF, atrial activity is continuously and chaotically accelerated (heart rhythm) and the ventricular response irregular. AF generates an action potential (electrical impulse) that travels along the cardiac cell membrane such as an electric discharge wave, modifying their distribution of charge, thus, cardiac arrhythmia being produced. [5] [18].

Unlike menthol that acts as cough suppressant, antiarrhythmic drugs are not suppressive of arrhythmia. They don´t work by calming irritable areas. In fact, most of them work by simply changing the shape of the cardiac action potential produced in the AF. These drugs mainly alter the conductivity and refractive capacity of the cardiac tissue. In consequence, control of arrhythmia is achieved by modification of the electrophysiological characteristics of the reentrant circuits, *i.e.* electrical transfer between cardiomyocyte cells generate the cardiac arrhythmia, so that the occurrence of reentries of electrical signals is less likely [18] [19].

The implementation of “upstream therapies” to prevent or delay myocardial remodeling is an attractive approach in the prophylaxis and treatment of arrhythmias associated with heart failure (cardiomyopathy) or myocardial infarction (coronary artery disease). Potential medications in this category include anti-inflammatory agents, inhibitors of the renin-angiotensin-aldosterone system, omega-3, polyunsaturated fatty acids, statins and antifibrotic agents.

Most of the positive results with the “upstream therapies” come from experimental models, observational studies and retrospective analysis of clinical data, whereas the prospective randomized trials have not shown a beneficial effect in the secondary prevention of the burden of AF or in cardiovascular outcomes. This fact might be explained because “upstream therapies” are effective at the beginning of the remodeling process, but ineffective in later stages, when the established structural remodeling is irreversible, or because medications are only effective in patients with certain comorbidities [20] [21] [22] [23].

Clinic researchers have identified treatments directed to specific genotypes to prevent arrhythmias in patients with hereditary cardiomyopathies. For example, several studies have shown that patients with LQTS3 can benefit from sodium channel inhibition, where the reversion of the genetic defect by antiarrhythmic drugs can prevent atrial and ventricular fibrillation. However, it will require an integration between scientific and clinics studies to develop these concepts and to validate controlled multicenter trials. Such integration constitutes a great opportunity but is also challenging [24] [25] [26] [27] [28] [29].

Surgical procedures are frequently useful in the treatment of arrhythmias. The localization of reentrant circuits can be performed surgically using diagnostic catheters, introducers, cartography and visualization systems [30]. One of the main tools in an electrophysiology laboratory is based on reentrant circuits that can be interrupted by means of radiofrequency ablation [31]. The complexity of the procedure, the learning curve, potential complications (some fatal) and few hospital centers that have this capability generate a bottle neck that prevent the growth of the ablation technique in the treatment of chronic AF. These treatments are applied without considering the costs of reinterventions and the non-selective handling [32].

Intelligent Nanocarriers

Nanoparticles that transport drugs and imaging agents are increasingly common in clinical practice, but they are generally passive release vehicles. Active and intelligent nanoparticles have an important function to orientate a specific drug to the target tissue or cell. This allows nanoparticles to accumulate in the target tissue at higher concentrations, in comparison to nanoparticles without activity. In this way, the therapeutic efficiency increases and the side effects reduces [33].

Hoe Jin Hah and his research group have developed a nanoplatform, consisting on intelligent nanoparticles of polyacrylamide, where methylene blue was encapsulated inside.

Then, they were functionalized with a specific peptide on their surface, which guide them to the tumor cells [34] [35] [36].

Regarding specific molecules to cardiac cells, some domain transduction proteins with specificity to cardiomyocytes (CTP) [37], endothelial cells, myofibroblasts and ischemic cardiomyocytes [38] [39] have been identified. The protein CTP has been used for Shuai Lu and theirs collaborates to target quantum dots to stem cells [40]. Uma Avula and their group have also used the CTP to functionalize a nanoplatform to make ablation of cardiomyocytes for photodynamic therapy [7] [8]. Siva Sai Krishna Dasa et al have developed active liposomes to release small molecules after myocardial infarction using the protein of ischemic myocardium [39]. Antibodies have been used to identify cardiac cells, they were implemented by Liu et al. to modify liposomes, thus orienting them to ischemic myocardium, for the treatment of arrhythmias [41]. In general, dendrimers, liposomes, polymer conjugates with drugs, microparticles, nanoparticles, nanomicelles, stent's with nanocoatings and intelligent microbubbles have been developed with the ability to locate a type of cardiac cell, through different types of bioreceptors [41] such as peptide ligand, antibodies and others targeting moiety groups (Figure 5).

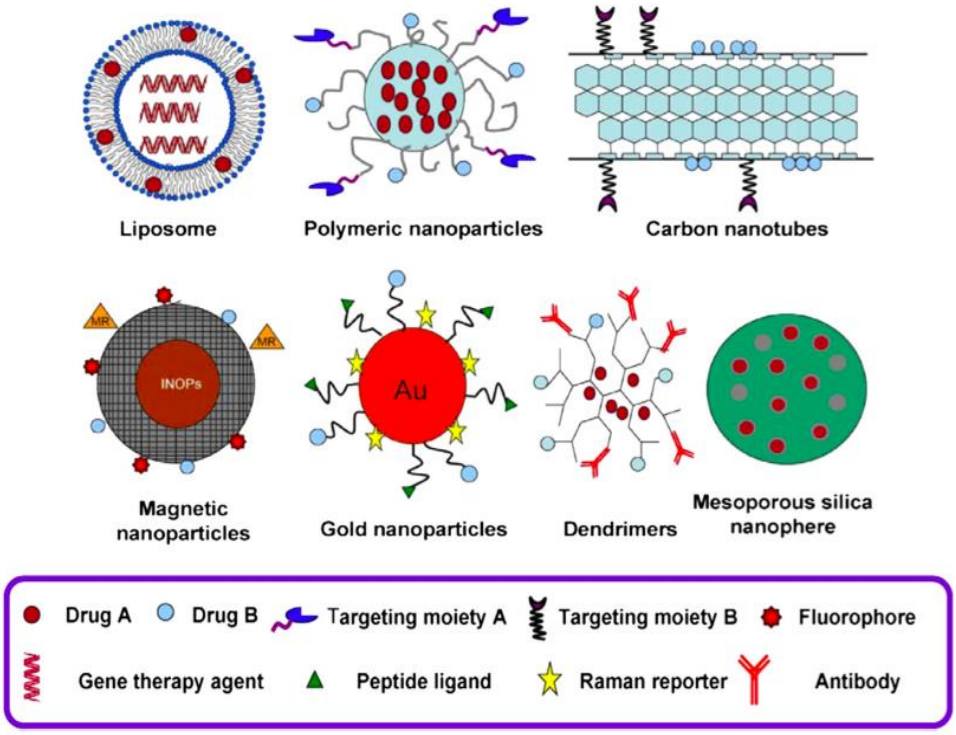

Figure 5. Intelligent Nanocarriers. Reproduced from [42].

Photosensitive Nanocarriers

There are nanoparticles that have the capacity to respond to different stimulus, thereby holding considerable potential for controlled release of drugs, it is therefore, an application that seeks to increase the temporal specify in the in-vivo release of drugs. These nanoparticles have the capacity to produce physicochemical changes, thus, they regulate the distribution of drugs in a specific time, when, they are exposed to some external stimuli. Such stimuli is applied based on the differences between the tumor ambient [43] and the normal tissue and comprises pH changes, proteases expression and external condition changes such as application of local heat, ultrasound, light, [44] magnetic and electric field [45] [46], etc. These systems capture a local stimuli or pathological change in the tissues and use it as trigger [47]. There are different types of nanocarriers that have been used for release of drugs, including dendrimers, liposomes, solid lipid nanoparticles, polymer-drug conjugates, peptide nanoparticles, micelles, nanoemulsions, nanospheres, carbon nanotubes and gold nanoparticles, etc. [36] [48].

Light has been commonly used as an external stimulus, due to its excellent space-temporal control of the cargo release into a cell or tissue. There are a plenty of photosensitive systems reported in the literature that exhibit response to light of different wavelengths. For example, properties of the systems change after exposition either to the ultraviolet, visible or near infrared radiation [36]. The light sensitive polymers are conformed by photoactive groups such as azobenzenes, spirobenzopyrans, triphenylethane or cinnamonil that may experience structural changes upon exposition to ultraviolet and visible light [48]. Changes of particles charge, size and form depend on photosensitive molecular groups that may be present in the light sensitive molecular structure and are triggered by different mechanisms. For example, the azobenzenenes and their derivatives are among the more studied photoactive groups. They suffer a reversible photoisomerization from CIS to TRANS on the sides of its nitrogen double bond. The ultraviolet radiation runs this isomerization, which can be reconverted to the TRANS isomer by visible light [36]. In this manner, nanospheres [49] [50] [51] and nanomicelles [52] [53] from azopolymers have been extensively developed.

NIR irradiation may alter the polarity of nanocarriers by producing an irreversible photorupture of some chromophores functionalized in the nanocarrier structure, for example, the 2-diazo-1,2-naphthoquinone. Such rupture generates destabilization of the nanostructures, with the concomitant release of some pre-incorporated cargo (drug). Other chromophores such as coumarin, pirenilmetil esters, silveneos, ditienileteno and o-nitrobenzil respond to ultraviolet, visible and near infrared. They may have structural or phase changes that may cause the release of the drug [54]. Different types of materials have

been developed with these chromophores to release drugs, such as photodegradable hydrogels, copolymers, thin films, self-assembled monolayers and bioconjugates [53] [55]. In particular, the researchers Jie Cao and theirs collaborators have used the o-nitrobenzyl for the fast and controlled release of drugs, through NIR photoactivable nanomicelles [56] and labeled polypeptides for orienting them to sugars in the development of cancer cellular therapy [57] or prodrugs [58].

The resultant nanobioconjugates from this project represent a great contribution to the development of therapies to control cardiac arrhythmias and others cardiac pathologies, due to there is not a research work that reports a specific therapy at spatial, temporal and cellular level. The state-of-the-art lack reports on photosensitive polymeric nanocarriers with specify to cardiac cells and the one reported here represent a great opportunity for this purpose.

CHAPTER III:

SELECTION AND MODIFICATION OF THE BIORECEPTOR

3.1 Introduction

There has been an intensive research in the development of nanoparticles as effective drug delivery systems for medical practice, especially for chemotherapy and gene delivery. Nanocarriers have been functionalized by conjugating them with a specific bioreceptor such as an antibody, a specific ligand and a transmembrane peptide. This functionalization allows the drug to be site-specific delivered to the desired target cells. Active targeting has demonstrated to significantly increase the nanocarrier specificity and efficacy.

Bioreceptors to target cardiac cells have been studied based on their capability to rich the cardiomyocytes cellular membrane. In this context, the cardiac targeting peptide (CTP) has been selected herein as the bioreceptor of the NBc for their demonstrated capacity to be internalized by the cardiac cells [8]. Furthermore, a FITC-linked CTP was used to facilitate their characterization by UV-microscopy. UV spectrum of the PNcs and FITC-CTP were recorded in order to determine the maximum absorbance wavelength.

3.2 Objective

- To select a specific bioreceptor with affinity to cardiomyocytes.

3.3 Methodology

Materials

The FITC-Cardiac Targeting Peptide (FITC-CTP) was commercially acquired from the GenScript (China) Company.

Bioreceptors selection

Antibodies, specific ligands and transmembrane peptides are the most frequently used bioreceptors to functionalize nanocarriers for targeting cardiac cells. Herein, the first objective was to select the more suitable bioreceptor among these three options.

Antibodies are immunoglobulins, [1] large proteins with shape of Y, produced mainly by plasma cells, that are used by the immune system to neutralize pathogens. Each tip of the "Y" of an antibody contains a paratope (analogous to a lock) that is specific to one particular epitope (analogous to a key-lock system) on an antigen, allowing these two structures to specifically bind together, with precision. Using this simple binding mechanism, antibody-functionalized nanocarriers have the capacity of targeting specific cells [59]. Antibodies have been used to identify cardiac cells and to modify liposomes, among other uses in biomedical science, thus holding potential to orient themselves to ischemic myocardium for the treatment of arrhythmias.

Specific ligands are substances that form a complex with a biomolecule to serve a biological purpose. In protein-ligand binding, the ligand is usually a molecule, which has the capability to produce a signal by binding to a specific site on a target protein. As proteins are the major structural component of cells and cell membranes, the specific ligands have affinity for the cells.

The transmembrane peptides are small bioreceptors that promote selective binding and effective internalization. Thus, 'cell-targeting peptides' (CTPs) connote a diverse group of molecules that have emerged from library screening, or by design, to bind to specific cell-surface receptors with high affinity and selectivity. Binding may or may not promote efficient cell entry, and therefore 'cell-penetrating peptides' (CPPs), another group of peptides, can enhance the transit of molecules or nanoparticles across membrane barriers. Use of CTPs and CPPs individually or jointly can provide with opportunities to enhance the capabilities and utility of nanocarriers [60].

Bioreceptor and photosensitive nanocarriers characterization

UV-spectrum of PNcs and FITC-CTP were measured to determine the wavelength of maximum absorbance between a range of 200 to 1000 nm. For this purpose, the Multiskan GO UV/VIS spectrophotometer was employed at "*Laboratorio de Proteómica*" from the Universidad Pontificia Bolivariana.

3.4 Results and Discussion

Selected Bioreceptor

CTP (Figure 6) was chosen as the bioreceptor because it is a transmembrane peptide with capacity to traverse the cellular membrane through the phagocytosis process [34]. This process is mediated by a receptor expressed at the cellular membrane that interacts with the CTP [6]. Besides, CTP has amine groups that can be linked to the surface of the photosensitive nanocarriers (PNcs) through the carboxylic groups that are present in their outermost surface. After PNcs functionalization, they can be internalized by the cardiac cells. Indeed, CTP has been used already to deliver cargoes to the heart, which would be of significant therapeutic potential for delivering small molecules, proteins and nucleic acids [58].

Zhid M (2010) and his work team have synthetized the CTP with the follow peptide sequence APWHLSSQYSRT, wich characteristics are described in Table 1, where the Acc No. is the reference number of the Pep Bank (Peptide Bank) of Harvard University.

Table 1. Peptide characteristics [37] [61] [62].

Type	**Peptide**
Name	Cardiac Targeting Peptide (CTP)
Acc No.	58211
Sequence	APWHLSSQYSRT
Origin	Phage Display
Isoelectric Point	9.95

The selected Cardiac Targeting Peptide molecule is depicted below.

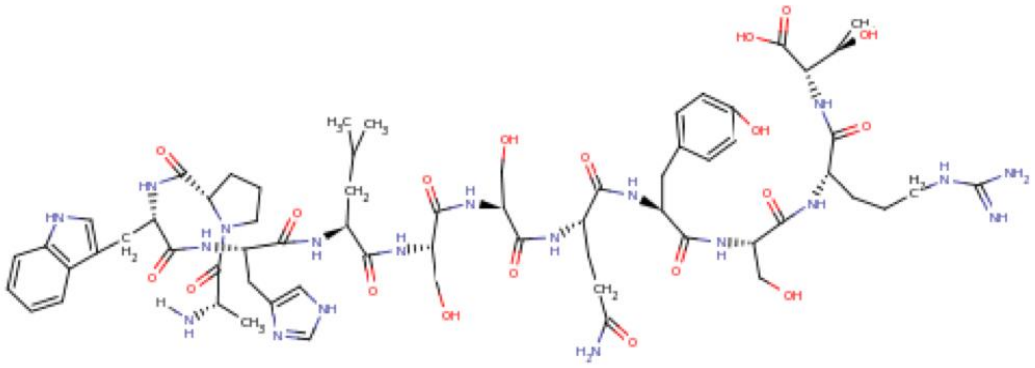

Figure 6. Cardiac Targeting Peptide. Reproduced from [61].

Modification of the bioreceptor.

The Cardiac Targeting Peptide was modified in the N-terminal, where fluorescein isothiocyanate (FITC) is functionalized (FITC-CTP); and the C-terminal was exchanged for an amine group. Functionalization with FITC and exchange at the C-terminal was performed to facilitate the CTP characterization through UV-VIS spectroscopy and the anchoring to the nanocarriers process, respectively (Figure 7). The CTP was commercially acquired from the GenScript company (China) and used as received.

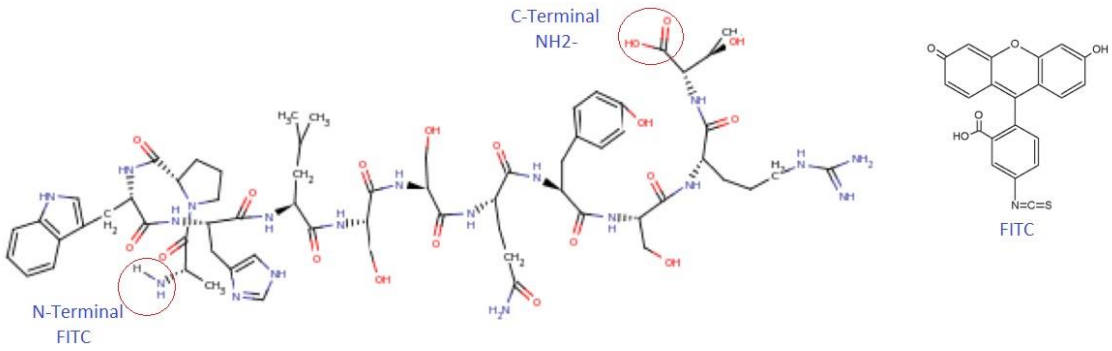

Figure 7. FITC- and NH_2-Modified Cardiac Targeting Peptide (FITC-CTP).

Bioreceptor and photosensitive nanocarriers characterization

The bioreceptor and photosensitive nanocarriers were characterized by spectrophotometry as detailed in the 3.3. Methodology section. The absorbance curves from Figure 8 show that whereas the photosensitive nanocarriers have a maximum response at 343 nm (black line), due to the presence of the azobenzene group, the FITC-CTP present its maximum at 492nm (blue line), corresponding to the weave length emission of the FITC chromophore (Figure 8). The spectrum was further used to estimate the concentration of the FITC-CTP-functionalized PNcs as will be shown in Section 4.4.

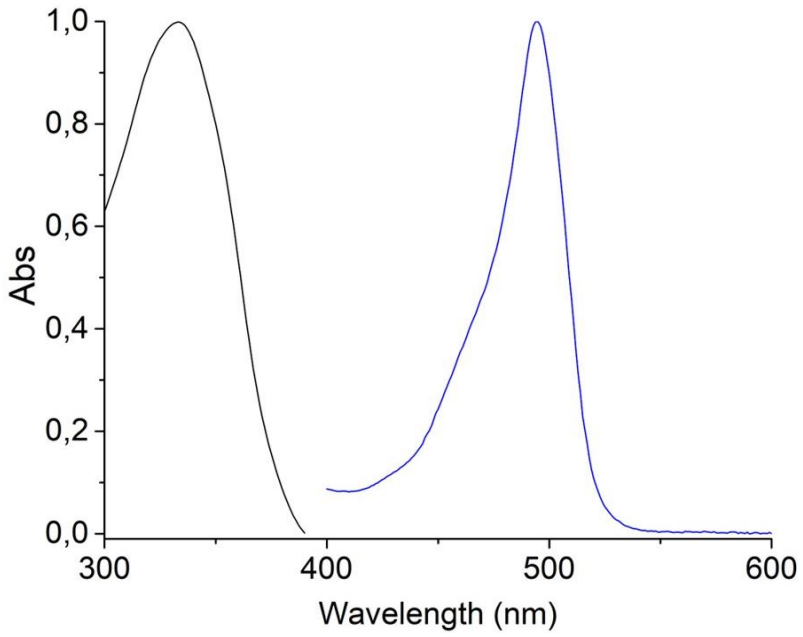

Figure 8. Maximum absorbance wavelength of Photosensitive Nanocarriers (black line) and FITC-modified Cardiac Targeting Peptide (blue line).

The presence of the carboxylic groups on PNcs makes the particles susceptible of being linked with amino-containing bioreceptors such as the one from of the FITC-CTP. Thus, covalent linking between the (PNcs) and the CTP through the standard EDC/NHS chemistry is feasible.

3.5 Conclusions

- The Cardiac Targeting Peptide was selected as the bioreceptor with affinity to cardiomyocytes because of its demonstrated ability to be internalized in the cardiac cells, through the endocytosis process.

- The CTP was modified with FITC at the N-Terminal, to be able to be characterized by UV-Spectroscopy, and the C-Terminal with amine groups to be anchored at the surface of the PNcs.

- Covalent linking between the (PNcs) and the CTP can be easily achieved through the EDC/NHS chemistry.

- The maximum emission weave length of PNcs and FITC-CTP at 492 and 343 nm, respectively made possible the quantification of the concentration of FITC-CTP-functionalized PNcs, through UV- VIS spectroscopy.

CHAPTER IV:

ASSAMBLY OF PNcs-CTP NANOBIOCONJUGATES: DESIGN, IMPLEMENTATION AND CHARACTERIZATION.

4.1 Introduction

Nanoparticles functionalized with specific bioreceptors (active nanoparticles) are the future of the therapies to treat diseases that use pharmacotherapy. Nanoparticles have capacity to orientate a specific drug towards the target tissue, thus, increasing the therapeutic efficiency whereas reducing the side effects [33]. There have been different treatments developed to fight the AF. For example, cardiomyocytes ablation (by photodynamic therapy) using a polyacrylamide nanoparticles nanoplataform-encapsulated methylene blue, functionalized with CTP demonstrated to increases the efficiency of the ablation process [7] [8].

In this chapter, a new active nanoparticle (nanobioconjugate) has been synthetized through conjugation of the PNcs and FITC-CTP and further functionalized with the CTP bioreceptor. The development expect to circumvent the necessity of releasing antiarrhythmic drugs instantly and site-specific in cardiac cells [7]. The morphology, particle size, charge concentration and fluorescence of the PNcs and NBc were characterized by SEM, TEM, DLS, z potential, UV-vis spectroscopy and confocal microscopy.

4.2 Objectives

- To design and to implement the protocol for functionalization of the photosensitive polymeric nanocarriers with the CTP specific bioreceptor (assembly of a Nanobioconjugate).

- To characterize the as-prepared functionalized photosensitive nanocarriers with the specific bioreceptor.

4.3 Methods

Materials

FITC-CTP: The FITC-Cardiac Targeting Peptide (FITC-CTP) was commercially acquired from the GenScript company (China).

All reagents were commercially acquired from Sigma-Aldrich (USA):

1-Ethyl-3-(3-dimethylaminopropyl) carbodiimide (EDC): CAS Number: 1892-57-5, reference: 39391.

N-hydroxysuccinimide (NHS): CAS Number: 6066-82-6, reference: 130672.

Phosphate Buffer Saline (PBS): This solution was prepared using:

HCl: CAS Number: 7647-01-0, reference: 320331.
NaOH: CAS Number: 1310-73-2, reference: 795429.
NaCl: CAS Number: 7647-14-5, reference: 746398.
KCl: CAS Number: 7447-40-7, reference: 746436.
Na_2HPO_4: CAS Number: 7558-79-4, reference: NIST2186II.
KH_2PO_4: CAS Number: 7778-77-0, reference: PHR1330.

2-[4-(2-hydroxyethyl)piperazin-1-yl]ethanesulfonic acid (HEPES): CAS Number: 7365-45-9, reference: H3375.

Tween 20: CAS Number: 9005-64-5, reference: P1379.

Nanobioconjugate Assembly

The Nanobioconjugate was obtained by modifying the methodology published by Sehgal [63] and Lu (2010) [40]. 1-Ethyl-3-(3-dimethylaminopropyl) carbodiimide EDC and N-hydroxysuccinimide (NHS) were used to activate the carboxyl-terminated groups from the outermost PNcs surface, for conjugation with primary amines from the peptide. Such activation generates a succinimide derivate, that being a very good leaving group is easily replaced by the amino moiety from the bioreceptor. The reaction is performed in 2 steps as detailed as follow.

1. *Activation step (EDC/NHS)*

Activation of the carboxylic groups on the surface of PNcs was achieved by incubation of 50 µl of the as-prepared PNcs in 100 µl (2mg/ml) of a phosphate buffer saline (PBS) solution prepared by diluting 1.9 mg EDC (20 mM) and 2.1 mg NHS (40 mM) in 500 µl of 25 mM 2-[4-(2-hydroxyethyl)piperazin-1-yl]ethanesulfonic acid (HEPES) buffer solution pH 6.5, for 30 min and washing only once with 100 µl of HEPES buffer.

2. *Covalent binding*

Functionalization of the FITC-CTP with activated carboxylic groups from the PNsc, by incubation 100 µl of the activated PNcs in 0.05 M phosphate buffer saline solution (PBS) to pH 9.8 (unless other buffer specified by the provider and always around the isoelectric point of the peptide, see Figure 1), containing 250 µg/ml FITC-CTP, for 2h. Washing the functionalized PNcs with 100 µl of pH 7.4, PBS (1x), containing 0.05 % tween 20 (store at 4°C until use). To perform the experiments, the stored solution is centrifuged at 5000 rpm and resuspended in 100 µl pH 7.4, PBS (1x) (without tween). This reaction process is in the Figure 9.

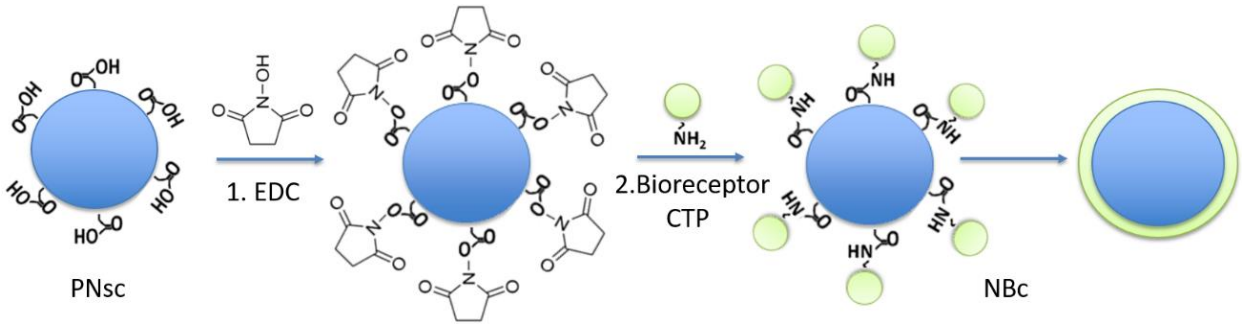

Figure 9. Synthesis of the NBc by covalent coupling the PNcs with the CTC bioreceptor through the EDC/NHS chemistry.

Characterization of the PNcs and NB

Morphological and microstructural characterization

A JEOL JSM 6490 LV SEM with ultra-high vacuum chamber was employed to characterize the morphology of the PNcs and NBc.

FEI Tecnai G2 20 transmission electron microscope, LifeScience Microscopy Facility was used to characterize the morphology of the PNcs and NBc.

Histograms of the particles size were plotted with values from the image J program, using the SEM and TEM images.

Particles size and charge.

Particle size distribution and polydispersity index were determined in aqueous solutions, at room temperature, using the Malvern Zetasizer Nano-ZS analyzer. Where, the hydrodynamic diameters of the PNcs and NBc were calculated according to the Stokes-Einstein equation. Each measurement was done in triplicate, with 100 cycles each.

Nanoparticles (PNcs and NBc) surface charge was determined by analyzing samples in aqueous solutions, at room temperature, employing the Malvern Zetasizer Nano-ZS equipment. Each measurement of PNcs and NBc were done in triplicate and the measurement averaged.

Concentration of PNcs and NBc

Absorbance-concentration dependence curves were recorded by spectrophotometry using a Multiskan GO UV/VIS, in a wavelength ranging from 200 to 1000 nm. From the spectra, the maximum intensity values obtained at 343 and 492 nm for the PNcs and FITC-CTP, respectively were used to plot two calibration curves that show the correspondent absorbance-concentration dependence.

To determine the concentration of peptide functionalized on the surface of the PNcs, two curves of absorbance with respect to concentration at 343 and 492 nm for PNcs the FITC-CTP, respectively were plotted through UV-VIS spectroscopy (Figure 15).

An excess of CTP was used in the reaction to assemble the NBc, named the initial solution. After the reaction, the remained not functionalized CTP was removed by centrifugation at 5000 rpm for 10 minutes. Both, the resultant NBc and the free FITC-CTC in the supernatant were then collected. The centrifuged was resuspended in a known volume, thus, the concentration of PNcs and FITC-CTP can be calculated by using the equations (1) and (2), respectively by subtracting the obtained amount from the initial one.

Fluorescence of PNcs and NBc

Confocal microscope was used to verify if the PNcs and NBc have fluorescence. For this purpose, filters from 620 nm to 700 nm (red), 495 nm to 515 nm (green) and 450 to 490 nm (blue) were used.

4.4 Results and Discussion

Morphological and microstructural characterization

The as-prepared photosensitive nanocarriers and nanobioconjugates were morphologically and microstructurally characterized by SEM and TEM images.

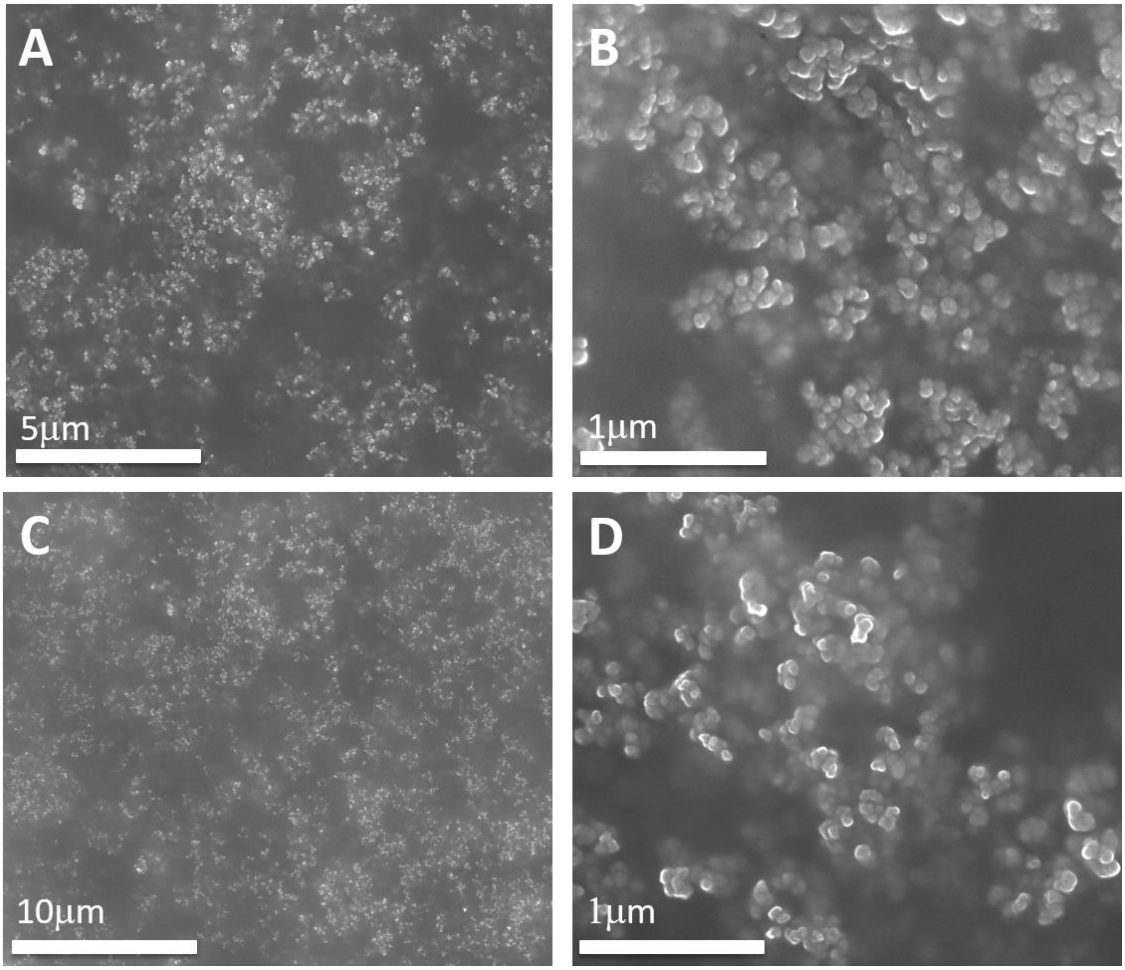

Figure 10. SEM images of PNcs (A and B) and NBc (C and D), from lyophilized samples. Scale bare are 5 (A), 10 (C) and 1 μm (B and D), respectively.

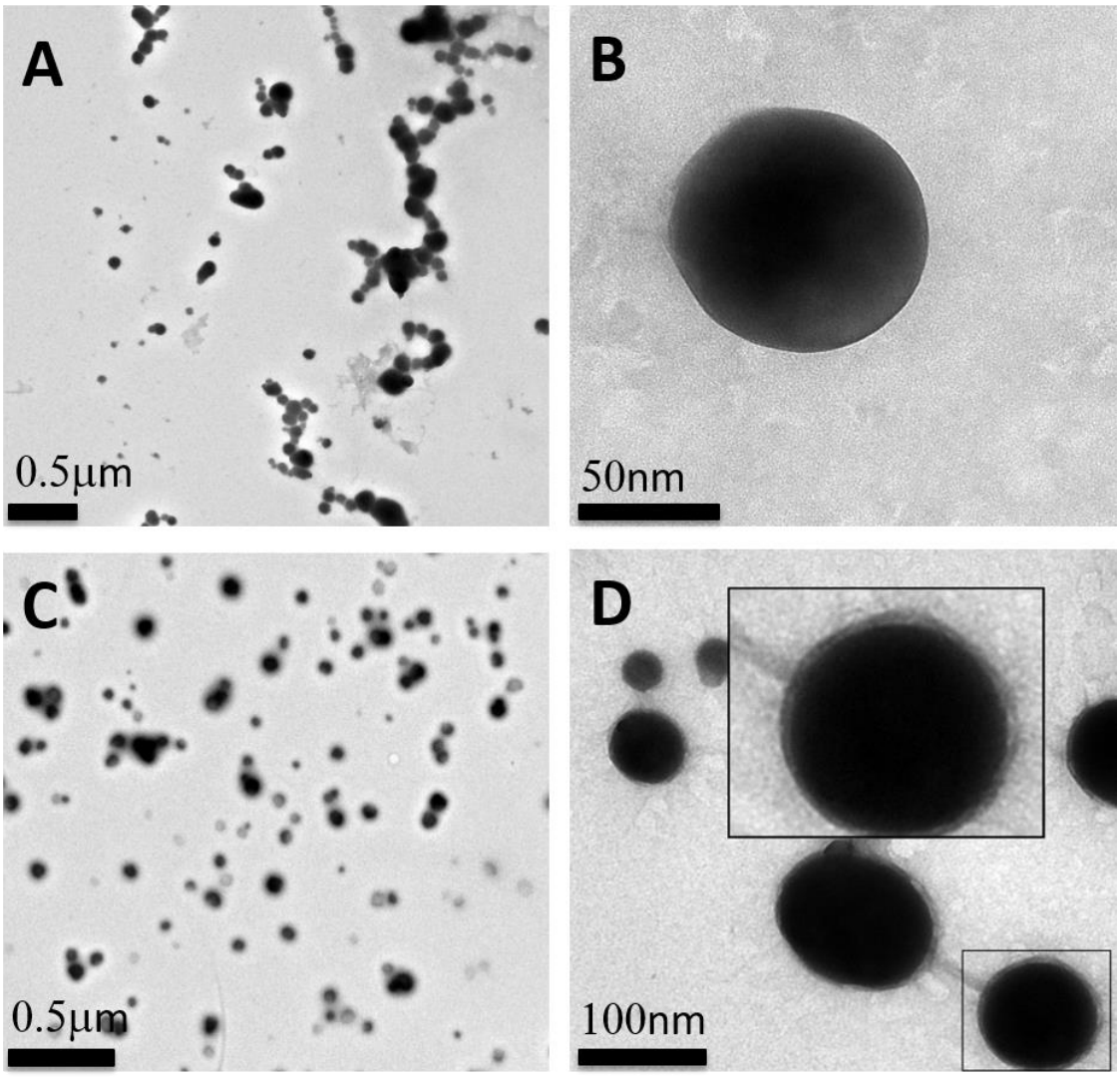

Figure 11. TEM images of PNcs (A and B) and NBc (C and D). Scale bare are 0.5 µm (A and C) and 50 nm (B and D).

SEM images from Figure 10 show that the PNcs have a spherical shape (A and B) and the NBc (C and D) keep the spherical morphology when the CTP is coating their surface. Histogram of the particles size in Figure 12 shows 64.09 ± 15.82 and 67.90 ± 13.79 nm mean size of the PNcs and NBc, respectively.

Some TEM images were taken to have a more precise idea about the size of the PNcs and NBc and confirm the PNcs functionalization. Figure 11 shows TEM images of the photosensitive nanocarriers at 0.5 µm (A) and 50 nm (B) scale bare, respectively; and the nanobioconjugate at 0.5 µm (C), and 100 nm (D) scale bar. Figure 12 shows a histogram of

the particle size distribution. The mean particle size was estimated to be 84.06 ± 33.06 and 99.07 ± 43.32 nm for PNcs and NBc, respectively. Results show not only that the CTP functionalized nanoparticles (NBc) have an apparent slightly higher size respect to the bare nanoparticles (PNcs and NBc), but also the sizes estimated by DLS were slightly higher than those measured by TEM, as expected. This later apparent discrepancy is related with the fact that DLS shows the dynamic radio of the particle and TEM allows to directly estimate the geometric ratio. Particles size from TEM images were also apparently higher than those form SEM images. This difference might be related with the fact that SEM samples were dried under high pressure through of a lyophilization process. Anyway, the functionalized NBc showed higher sizes respect to the correspondent PNcs counterparts, thus indicating the functionalization process tuck place. The core/shell-like resultant structure depicted in Figure 11D is another indication that the PNcs were properly functionalized with the peptide. The darker inner part corresponds to the polymeric particle coming from the staining (as detailed in the experimental section) and the little cleared thinner part is the peptide. Indeed, the modified PNcs is completely covered by an "halo" that indicates the surface coverage extend is high.

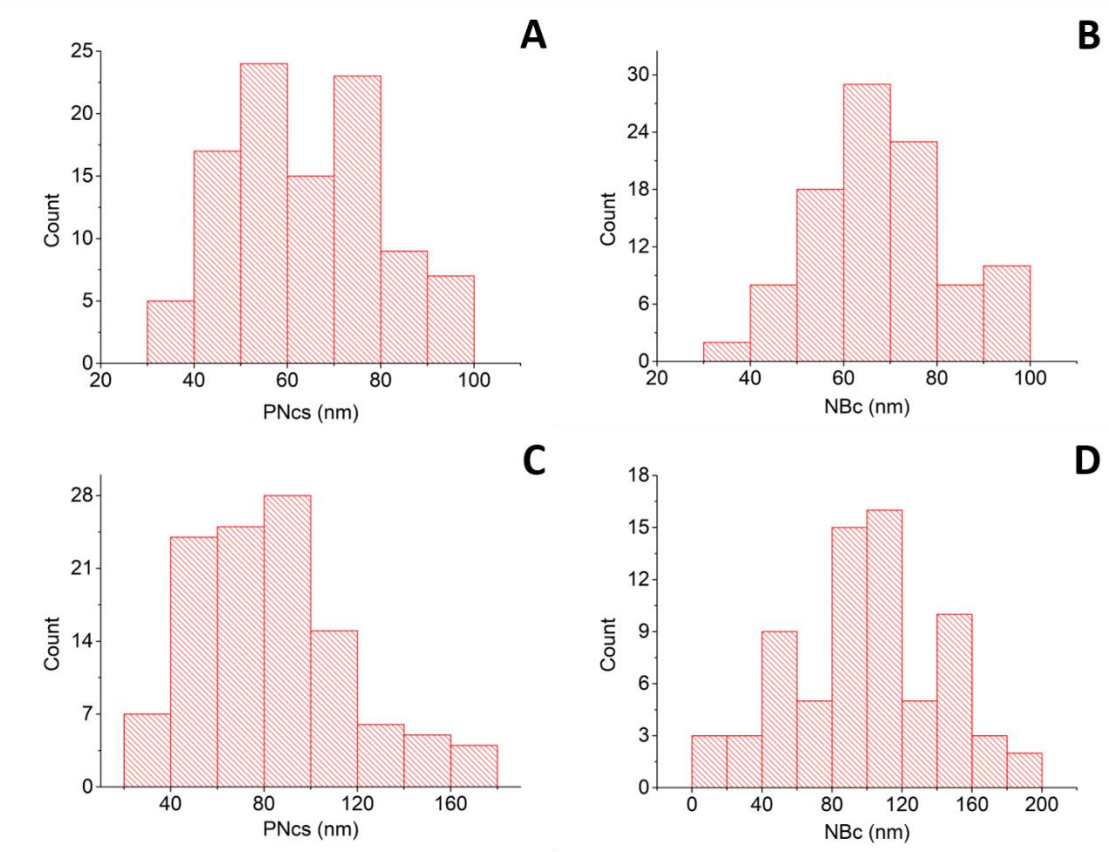

Figure 12. Histogram that show the size particle distribution from SEM images (A and B) and TEM images (C and D).

Particles size and charge

Particles size of the photosensitive nanocarriers and nanobioconjugates were estimated by DLS, which get an insight about PNcs dynamic radius and how it shifts towards higher values after FITC-CTP functionalization (NBcs). Figure 13 shows a plot of particle size distribution. Based on the results, the PNcs average dynamic radio is 91 nm and it shifts about a ten after the functionalization process. The shift is an indication of the functionalization process occurred. Apparently, the size of PNcs seems to be optimal to be endocited by the cardiomyocyte cells. It is know that nanoparticles size of about 100 nm can potentially pass through the cellular membranes [40].

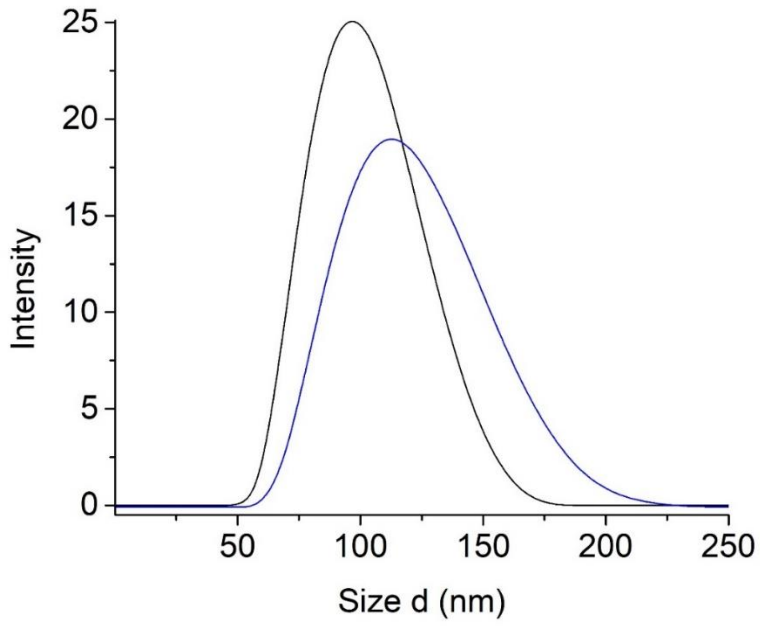

Figure 13. Estimation of particle size by DLS, for photosensitive nanocarriers (black line) and nanobioconjugates (blue line).

Surface charge of the PNcs and NBc were then determined as a way to confirm that the functionalization process happened. Figure 14 shows an increase in the z potential when PNcs are functionalized to produce the NBc.

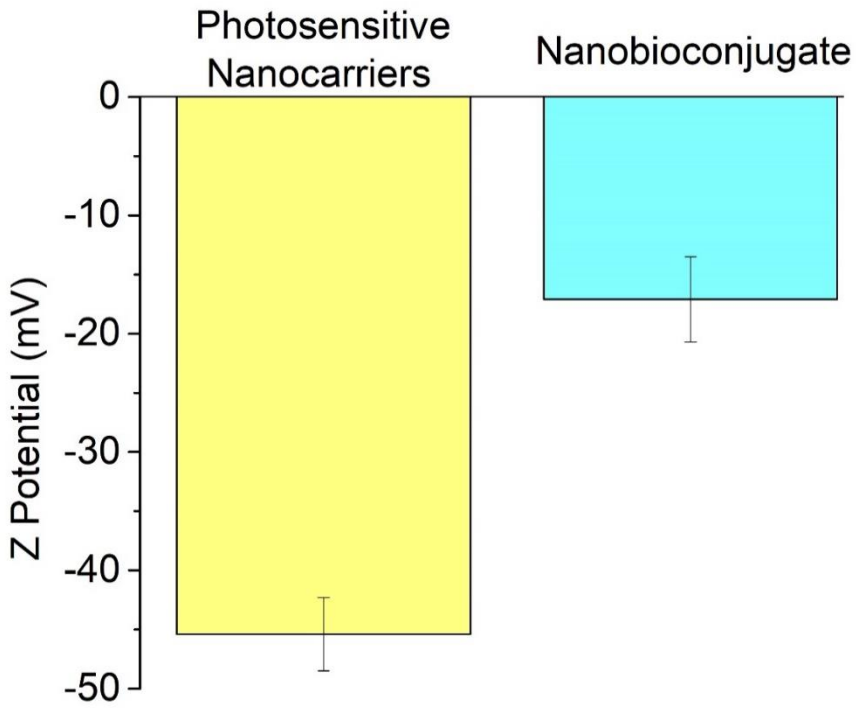

Figure 14. Surface charge of photosensitive nanocarriers and nanobioconjugates.

The z potential of the PNcs is -45.4±3.1 mV, which indicates that PNcs are stable in solution (absolute value much higher than -30 mV). The reason why the z potential is significantly negative is related to the presence of carboxylic groups at the outermost nanocarriers surface, indicating that when they are dispersed in an aqueous medium, such moieties are mostly ionized. When PNcs are functionalized, forming the NBc, their z potential goes down to -17.1 ± 3.6 mV (Figure 13). Such change is a confirmation that the functionalization process happened. The carboxylic groups from the PNcs are likely coupled to the primary amines from the CTP (Figure 9), thus changing their surface charge. The negative charge at the NBc surface accounts for their stability in aqueous solutions.

Concentration of PNcs and NBc

Figure 16 shows the absorbance spectrums of the initial solution (black line), the supernatant (blue line) and centrifuged (red line) with maximum absorption peaks at 343 and 492 nm, which correspond to the self-fluorescence of the PNcs and the fluorescence from the FITC dye, respectively. From the maximum absorption peaks and tacking into account the initial concentration of CTP, it was possible to estimate the PNcs and FITC-CTP

concentrations, respectively by means of equations (1) and (2) from Figure 15, as detailed in the methods section. Estimation of the concentration of both PNcs and FITC-CTP-functionalized PNcs is shown in Table 2.

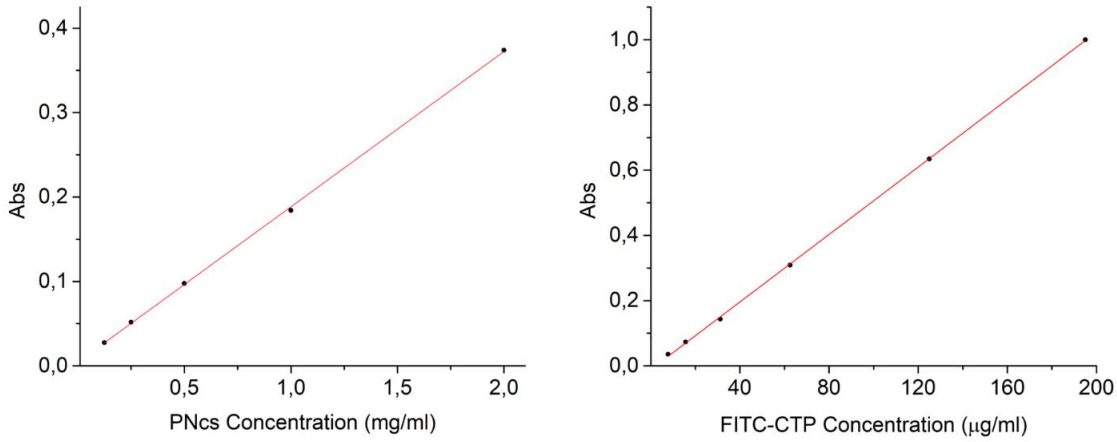

Figure 15. Absorbance and concentration curve of photosensitive nanocarriers and FITC-modified Cardiac Targeting Peptide.

Figure 15 (left side) is a plot of PNcs concentration-absorbance dependence, at 343 nm, ranging from 0.027 to 0.37 absorbance units, described by the linear equation 1, with a correlation coefficient (R^2) of 0.9997.

$$C\ of\ PNcs\ \left[\frac{mg}{ml}\right] = (Abs - 0{,}0044)/0.184 \quad (1)$$

Likewise, Figure 15 (right side) is a plot of FITC-CTP concentration-absorbance dependence, at 492 nm, ranging from 0.036 to 1.0 absorbance units, described by the linear equation 2, with a correlation coefficient (R^2) of 0.9998.

$$C\ of\ NBc\ \left[\frac{\mu g}{ml}\right] = (Abs - 0{,}011)/0.0052 \quad (2)$$

Where (1) and (2) have the form of following expression $x = \frac{y-b}{m}$, being x the concentration, y the absorbance, b the intercept and m the slope of the plots, respectively.

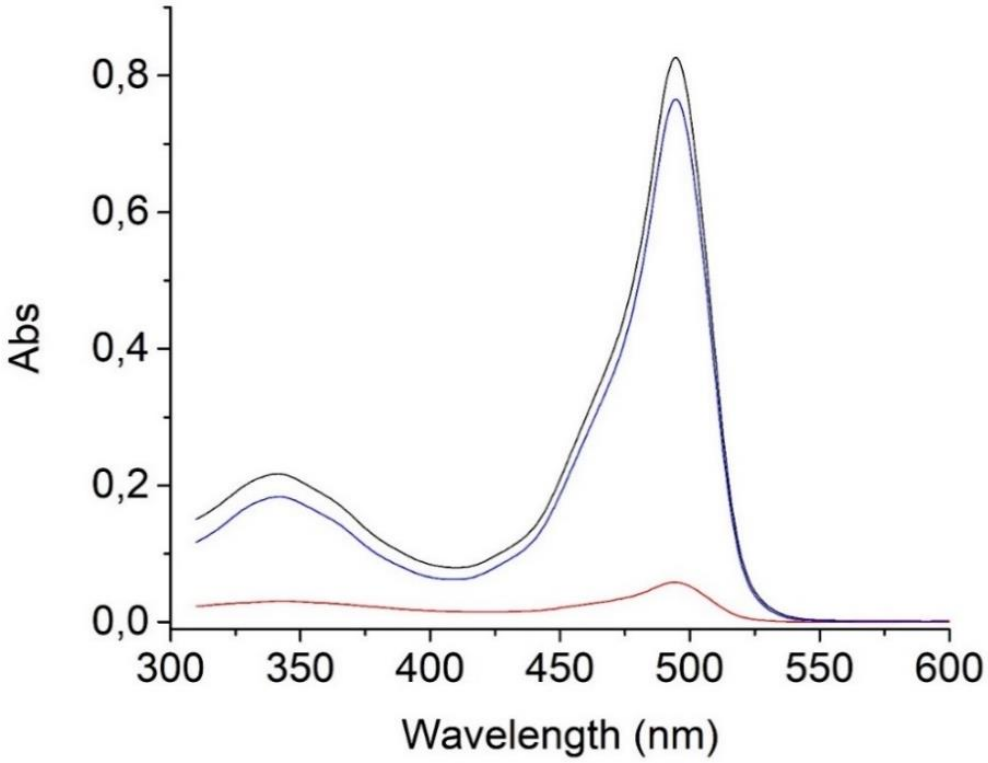

Figure 16. Concentration of FITC-CTP functionalized at the nanobioconjugates: Absorbance spectra of the initial solution (black line), the supernatant containing the free FITC-CTC that was not immobilized at the PNcs surface (blue line) and the centrifuged containing the FITC-CTP-functionalized PNcs (red line).

Table 2. Estimation of the concentration of both PNcs and FITC-CTP-functionalized PNcs.

Sample	**PNcs (343 nm)**		**FITC-CTP (492 nm)**	
	Abs	C[mg/ml]	Abs	C[μg/ml]
Initial	0,22	1,16	0,83	161,31
Supernatant	0,18	0,98	0,77	149,55
Centrifuged	0,03	0,14	0,059	13,65

Based on the results from Table 2, the NBc is composed of 0.14 mg/ml of PNcs, functionalized with 13.65 μg/ml of FITC-CTP, which corresponds to 95.63 μg FITC-CTP/mg

PNcs. This concentration seems to be reasonable, taking into account that the CTP must be a thin layer covering the surface of the PNcs, which is enough for internalization of the NBc in the cardiomyocyte cells, as will be demonstrated in Chapter 5.

Fluorescence of PNcs and NBc

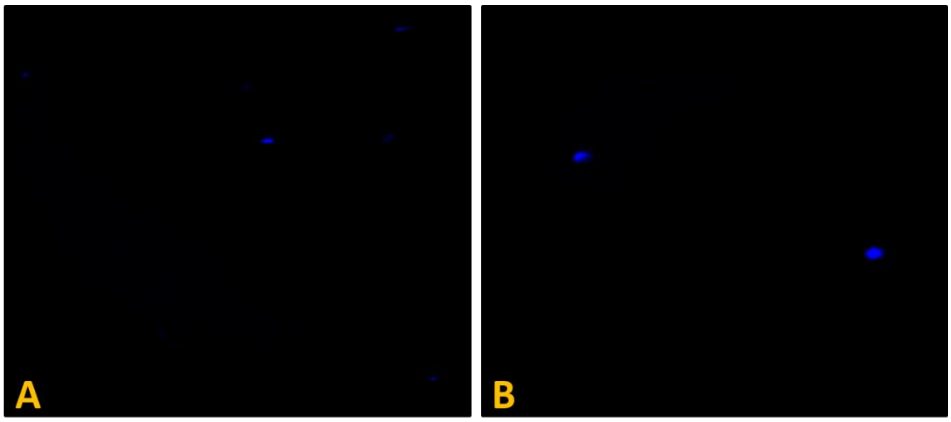

Figure 17. Confocal image of photosensitive nanocarriers (A) and nanobioconjugates (B), by confocal microscopy at 460 nm.

Confocal microscopy experiments demonstrated that the particles are autofluorescent at the 470 nm wavelength observed (Figure 17). Autofluorescence of both the azobenzene group and the N-Succinyl chitosan from the PNcs are the responsible of the particle autoflorescence (see Figure 1). Functionalized PNcs demonstrated to be also self-fluorescent as a result of the overlapping between the autofluorescence coming from the PNcs themselves and the one coming from the FITC-CTP. This characteristic will facility the characterization process as will be shown in the next chapter, where the specificity of the nanobioconjugates to cardiomyocytes will be evaluated. For this purpose, both nucleus and cytoplasm can be stained with fluorophores that emit at a wavelength different than 460 nm.

4.6 Conclusions

- Functionalization of the PNcs with the specific CTP bioreceptor was successfully achieved by the EDC/NHS chemistry.

- Effectiveness of the functionalization process was indicated by the shift in the particle size and z potential and confirmed by TEM when compared the PNcs and the NBs each other.

- Particle concentration and fuctionalization grade was quantitatively estimated.

- Both the PNcs and the NBs showed autofluorescence when interrogated by confocal microscopy.

CHAPTER V:

SPECIFICITY EVALUATION OF THE AS-PREPARED NANOBIOCONJUGATE TO CARDIOMYOCYTE CELLS

5.1 Introduction

The CTP has been linked with quantum dots to target stem cells, for gene delivery in regenerative medicine [40]. The CTP has been also linked to nanoparticles encapsulated photosensitizers to target cardiac cells to fight AF, through photodynamic therapy in cardiomyocytes [8] [37]. The NBc synthetized in the chapter IV has the potential to delivery antiarrhythmic drugs with a space-temporal specificity, to be used such as a new treatment against AF. These data demonstrate that the established method of screening for embryonic stem cell by specific binding peptides by phage display is feasible. Moreover, the peptide-conjugated quantum dots may be applicable for embryonic stem cell study and use.

In this chapter, the affinity (space-specificity) and biocompatibility (additional result) of NBc to cardiomyocytes will be demonstrated by confocal and fluorescence microscopy techniques and the MTT assays, respectively. The affinity was evidenced when the cellular area occupied for the NBc increased upon incubation time (8 h of incubation time are necessary to cover 15.9 % of cellular area with the NBc). The NBc was internalized into the cytoplasm of the cardiac cells by the endocytosis mechanism. The MTT assays showed the NBc biocompatibility, with a viable cell extent of 85 % at 24 h of incubation time.

5.2 Objective

- To evaluate the specificity of the active nanobioconjugate to cardiomyocyte cells.

5.3 Methodology

Materials

All reagents were commercially acquired from Sigma-Aldrich (USA):

DMEM supplemented with 10% (v/v) fetal bovine serum: Reference: D5796.

Calcein: CAS Number: 154071-48-4, reference: C0875.

3,3'-Dihexyloxacarbocyanine iodide (DIOC 6): CAS Number: 53213-82-4, reference: 318426.

Ethidium bromide: CAS Number: 1239-45-8, reference: E8751.

3-(4,5-dimethylthiazol-2-yl)-2,5-diphenyltetrazolium bromide (MTT): CAS Number: 298-93-1, reference: M2128.

Isopropanol: CAS Number: 67-63-0, reference: W292907.

The human fetal ventricular cardiomyocytes, RL-14 cells, are a commercially available cell line (American Type Cell Culture Patent Deposit Designation No. PTA-1499, Manassas, VA) that has been established from nonproliferating primary cultures derived from human fetal heart tissues. They used a mitochondrial function-based method to indirectly introduce the SV-40 gene into cells, which are normally intractable to standard transformation techniques [64] [65] [66].

Cardiomyocytes cultivation process

Human fetal cardiomyocytes cell line (RL14) was obtained from ATCC (PTA-1499). Cells with less than 17 passages were maintained in DMEM supplemented with 10% (v/v) fetal bovine serum at 37 °C, in a humidified atmosphere containing 5% CO_2. Biocompatibility assays were performed when cell cultures were at 80% confluence [67].

Internalization Time of PNcs and NBc in cardiomyocytes

The PNcs (or NBc) were added as treatments, at the same time, in 9 plates with cultivated cardiomyocyte cells. The cell cultures were characterized by confocal microscopy at different cultivation times, from 5 to 14 h for PNcs, where 5 hours does not present

internalization of NPs, and 6, 7 and 8 h for NBc (each h), respectively. These experiments allowed on one hand to establish the minimum time that the PNcs needs to be internalized in the cardiomyocytes through a phagocytosis process, and on the other hand the affinity of the NBc to the cardiac cells through an endocytosis process. Each image was taken 3 times for each culture, and the entire experiment was done in triplicate, then (n=9).

Area extend of PNcs and NBc inside the cardiomyocytes

Fluorescence microscopy images were processed with the image J program to quantify the cell area extent occupied by NBc and PNcs in the cardiomyocytes. Based on that, the cardiac cell area is 100%, and the nanoparticles (NBc and PNcs) area can be determined.

Characterization of the internalized PNcs and NBc

Design of experiments

Initially, a design of experiments is carried out by means of the statistical analysis software (SAS) program, by the blocks method, with three replies for each one.

Confocal Microscopy

Confocal microscope was employed to characterize PNcs inside of the cardiomyocyte cells. The cardiac cells were dyed with calcein that fluoresce between 495 and 515 nm (green) and the PNcs auto-fluoresces at 470 nm (blue).

Fluorescence Microscopy

Inverted microscope for research with bright field, DIC, and fluorescence (Ti-U Nikon Eclipse), equipped with a monochromatic camera (Nikon DS-Qi2 16MP USB 3.0), was used for fluorescence microscopy experiments. This microscope was employed to characterize the PNcs and NBc inside of the cardiomyocyte cells. Cytoplasm and nucleus of the cardiac cell were stained with DIOC 6, that fluoresces between 495 nm and 515 nm (green) and

with ethidium bromide, that fluoresce between 645 nm and 700 nm (red), respectively. PNcs and NBc autofluoresce at 470 nm (blue), the proper fluorescence wavelengths allowed to visualize the PNcs and NBc internalized in the cardiomyocyte cells.

In-vitro biocompatibility assays and cellular viability (additional results)

To assess the short-term cytotoxic effect of NBc on RL14 cardiomyocytes, MTT assay were conducted as an indicator of the metabolic competence of the cells [68], following the protocols reported in [69] and [70]. RL14 cells (4 x 10^3 cells/well, 96-well microplates) were incubated in 10 µl of 20 freshly prepared serial-dilutions (1: 2) of nanobioconjugate (from 2 to 0 mg/ml), for 24 h. At the end of the incubation time, 10 µl of MTT solution (5 mg/ml) was added to each well, the microplates were then incubated under constant stirring in dark for 6 h at 37 °C. 100 µl of cold isopropanol were then added to each well in order to dissolve the formazan crystals, followed by gentle stirring, in a gyratory shaker, for 12 to 24 h. After that, the optical density (OD) was measured with the Multiskan-go spectrophotometer, at a wavelength of 570 nm. In order to verify the results repeatability, three independent experiments were performed in triplicate. Also, positive (dimethyl sulfoxide, DMSO 100%) and negative (complete culture medium without cells) controls were also tested. Finally, the viability extent (VE) was determined using the equation 3.

$$VE = \frac{OD_{treated}}{OD_{-control}} * 100\% \quad (3)$$

Where, OD treated is obtained in the presence of PNcs and NBc treatments and OD-control is obtained from a untreated sample used as negative control [56] [34] [70].

5.4 Results and Discussion

Internalization Time of PNcs and NBc in cardiomyocyte cells

To evaluate the internalization of the PNcs and NBcs by the cardiomyocite cells, the PNcs were first incubated in the cardiomyocyte cells for 8 and 14 h. Figure 18 shows how we systematically observed and imaged this process by confocal microscopy. We first observed the very few blue spots from the self-fluorescent PNcs (A) at 470 nm, the cytoplasm was stained with calcein and observed with a 495-515 nm filter (B) and both of them merged (C)

after 14-h incubation time. The very little amount of PNcs that are able to penetrate the cardyomiocite cell membrane were evidenced in (D) even after a long incubation time of 8 h.

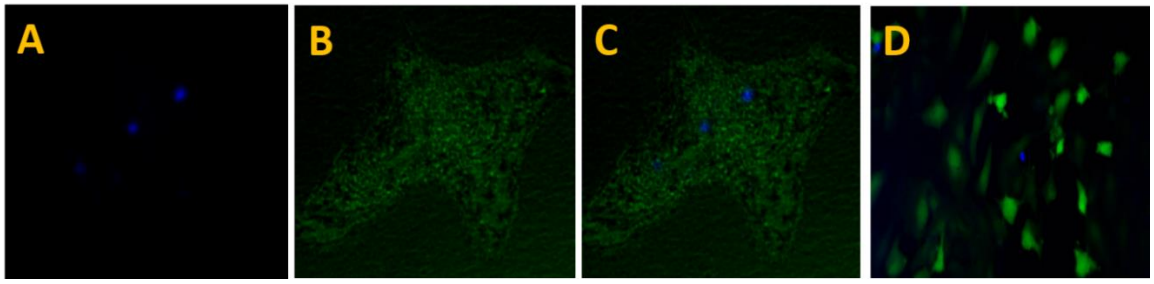

Figure 18. Confocal Microscopy images of low population of PNcs penetrating cardiomyocyte cells: only PNcs (A), Cardiomyocyte cell alone (B), and A and B merged after 14-h (C) and 8-h incubation time (D), respectively.

We later interrogated the internalization process of NBc in the cardiomyocyte cells for 5 (this time does not present internalization of NPs) , 6, 7 and 8-h and compared to that from the self-fluorescent PNcs incubated in the cells for 14-h. Figure 19 shows the fluorescence microscopy images of the cell nucleus stained with ethidium bromide (A), the cytoplasm stained with DIOC 6 (B), the self-fluorescent particles (C) and the three of them merged (D), by changing the internalization times of the NBc in the cardiomyocyte cells from 6 (b), 7 (c) and 8 (d) h, respect to the corresponding incubation of PNcs in the cells for 14 h (a), used as a control. Results demonstrated increasing number of NBc as incubation time goes with a dramatic increase after 8-h. NBc is internalized in the cardiac cells by the receptor-mediated endocytosis process, in which the cells engulf the CTP-coated nanoparticles by means of an energy-transforming active process. Herein, the cell internalizes the NBcs through an invagination of the cytoplasmic membrane, forming a vesicle that ends up detaching from the membrane to enter into the cytoplasm (Figure 19 and 20) [71]. See a sketch of the endocytosis process in Figure 20. In contrast, the PNcs are dramatically less internalized by the cells, in spite of the PNcs were incubated in the cells in an excess of 14-h (Figure 19a, from A to D). The PNcs may be internalized by phagocytosis, a variant of the endocytosis process in which some cells surround solid particles with their cytoplasmic membrane and introduce them to the cellular interior. This occurs thanks to the emission of pseudopods around particles or microorganisms to completely engulf them and form a vesicle around them, called phagosome, which subsequently fuse with lysosomes to degrade the phagocytosed antigen [71].

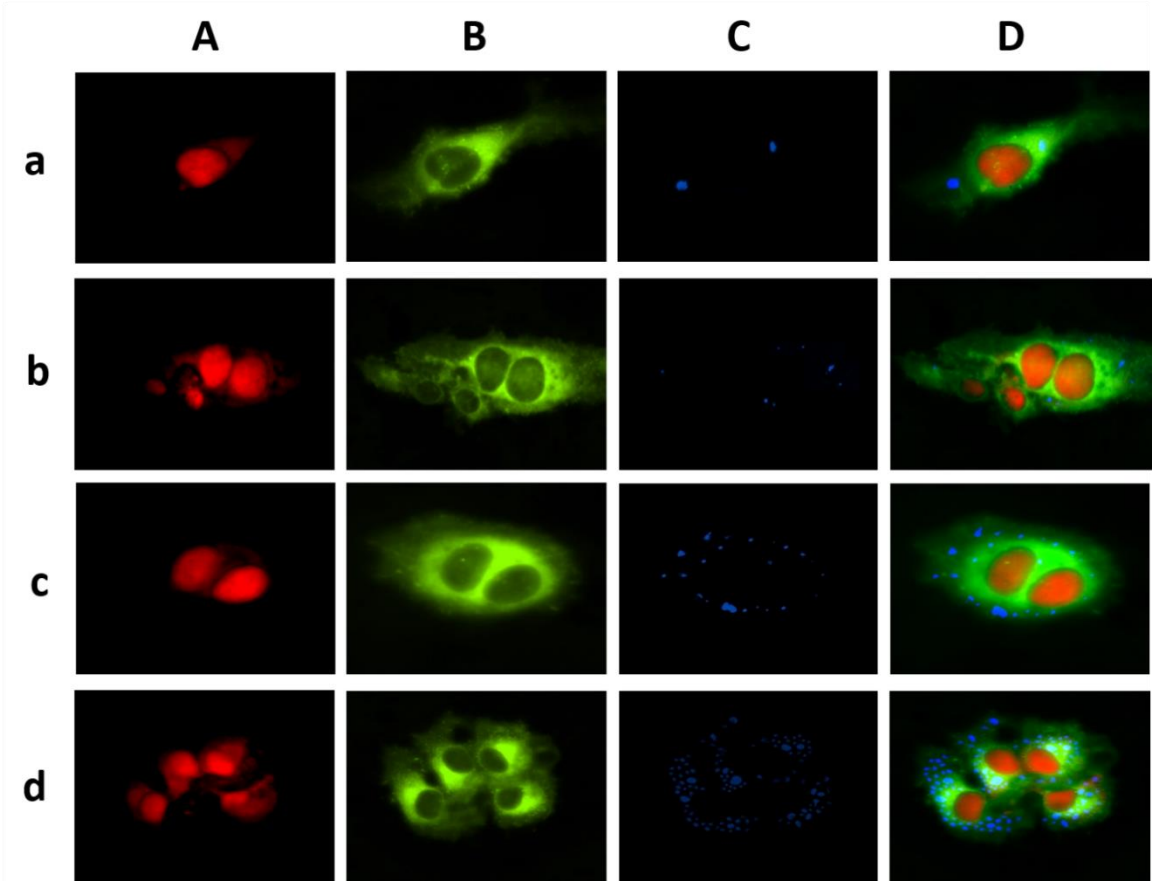

Figure 19. Fluorescence Microscopy images of the cell nucleus (A) the cytoplasm (B), the self-fluorescent particles (C) and the three of them merged (D), by changing the internalization time of the NBc in the cardiomyocyte cells from 6 (b), 7 (c) and 8 (d) h, respect to the corresponding incubation of PNsc in the cells for 14 h, used as a control (a).

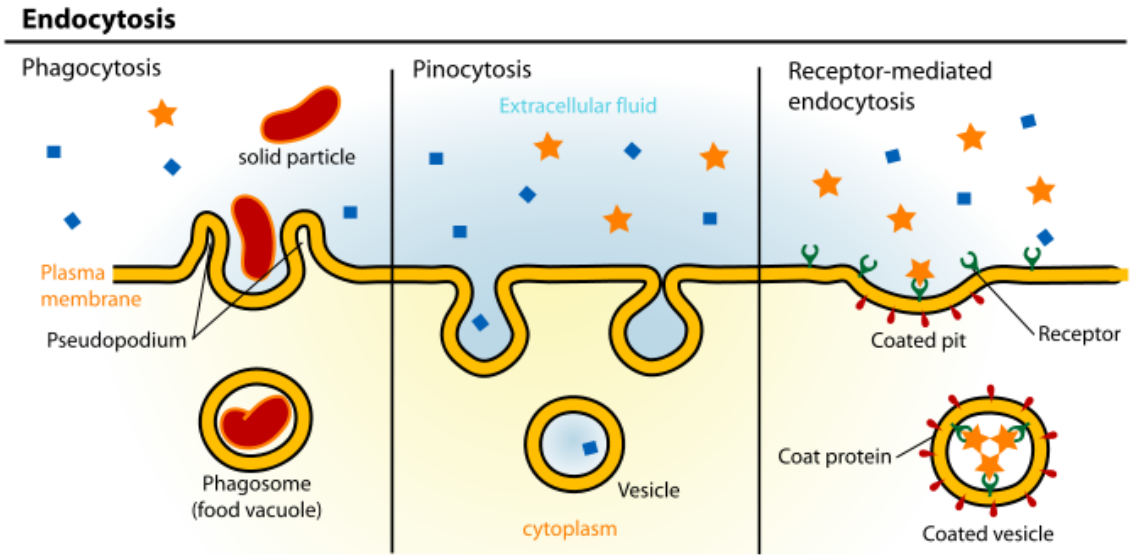

Figure 20. Phagocytosis (for PNcs, left side) and Endocytosis (for NBc, right side) process in Cardiomyocyte cells. Reproduced from [72]

To have an semiquantitative idea of penetration efficiency, the next set of experiments were dedicated to estimate the extent of the cardiomyocytes that were occupied by the PNcs and the NBc. Figure 21 illustrates the methodology used for this purpose. The total cellular area is artificially delimited, then estimated using the Image J software and determined as the 100 percent; whereas the nanoparticles (PNcs and NBc), estimated in the same way, correspond to the occupied area of the cardiac cells. The extent was calculated by a conversion factor with values estimated by triplicate, not only in three cells from the same cell culture, n=3 (Figure 22A) but also from 3 different cell cultures, n=9 (Figure 22B), to ensure the repeatability and reproducibility intra and inter cell culture.

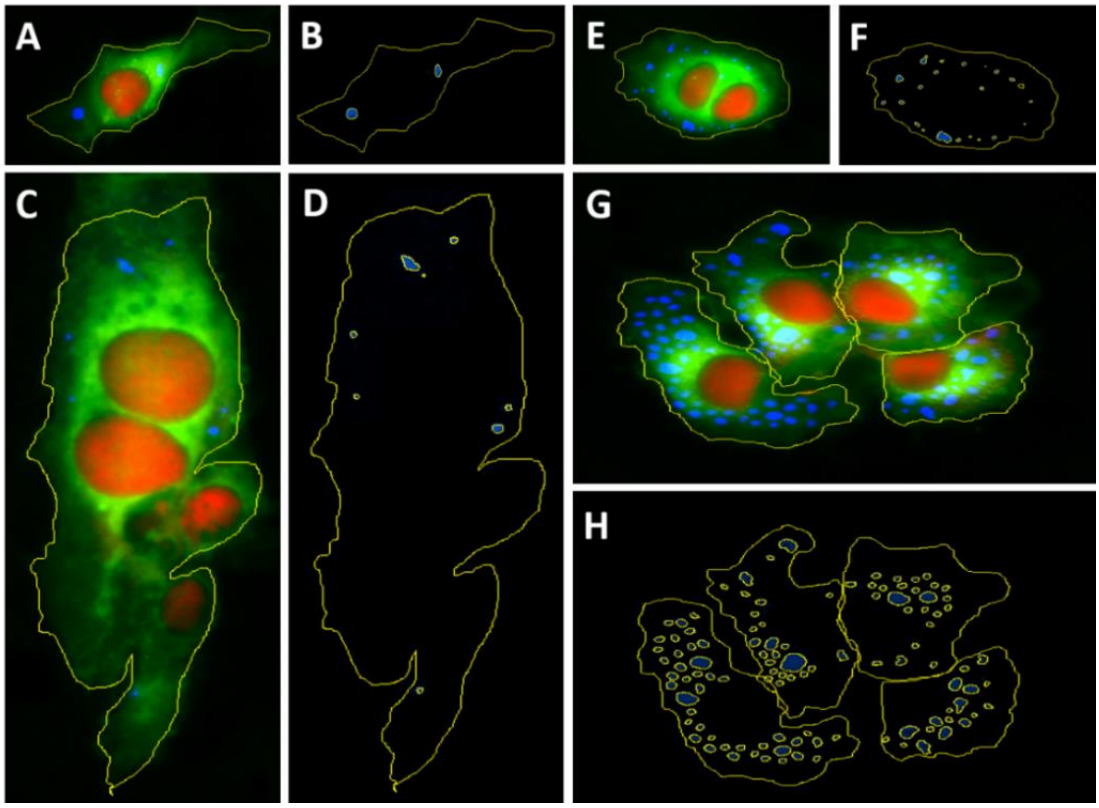

Figure 21. Methodology to estimate the extent of cardiomyocytes that were occupied by PNcs and NBc from the fluorescence microscopy images. Selection of cellular area (A, C, E and G), PNcs area in A (B), and NBc area in C (D), in (F), and in G (H), respectively.

The affinity of NBc for cardiomyocyte cells was demonstrated by estimating the increase of their occupied extent in the cardiac cell upon incubation time. There were significant differences between the hours of internalization (Num DF=4 , Den DF=30, F=3488.07, P<0.0001). No significant interaction was observed between the blocks of evaluation and the hour of internalization suggesting the reproducibility of the experiment (Num DF=8, Den DF=30, F=0.88, P=0.99). Figure 22B (n=9) shows that at the first internalization time tested (6 h), the area of NBc in the cells was only (n=9) (0.83 ± 0.02)%, which is similar to the internalization time of the PNcs in an excess of 14 h, used as a control (0.81 ± 0.03)% (DF=30, t-value=0.09, P=1.00). The internalization extent of the NBC slightly increases at 7 h incubation time (2.28 ± 0.04)% compared to 6 hours (DF=30, t-value=-9.03, P<0.0001). However, it experienced a dramatic increase of 5-fold, up to (15.90 ± 0.09)%, at 8 h, respect to that from 7 h incubation time (DF=30, t-value=-84.6, P<0.0001). These results demonstrated again the great affinity of the NBc for the cardiomyocyte cells (to see supplemental results).

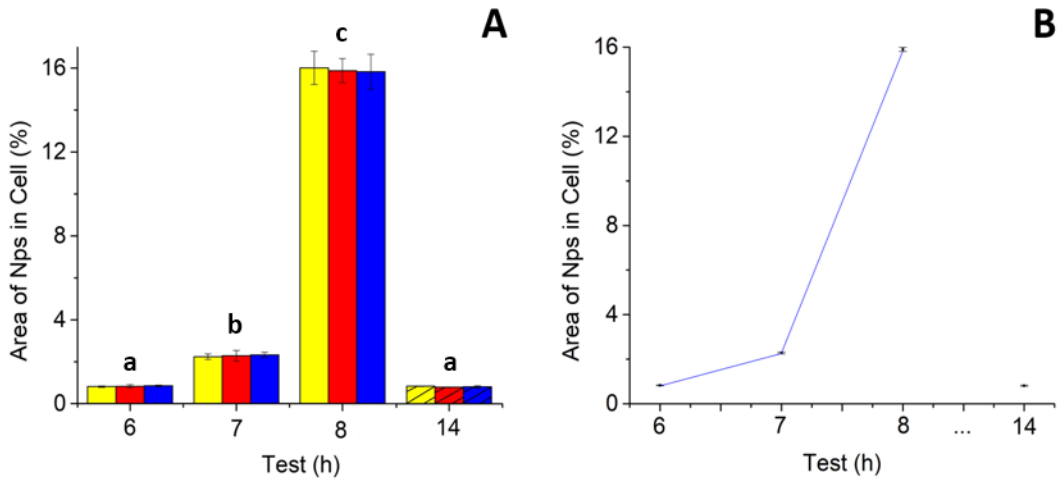

Figure 22. Nanoparticles extent internalized in the cardyomyocite cells at different incubation time. The average of triplicate tests at 6, 7 and 8 h (NBc), respect to 14 h (PNcs). The extent was calculated by a conversion factor with values estimated by triplicate from three cells from the same cell culture, n=3 (A) and from 3 different cell cultures, n=9 (B). Different letters correspond to significant differences at <0.001 between treatments using a TukeyHSD test for mean comparison.

In-vitro biocompatibility assays for cellular viability (additional results)

Cytotoxicity of the RL14 cardiomyocytes cell line induced by the NBc was assessed after treating cardiomyocyte cells with six successive dilutions of NBc from 0 mg/ml (the control) to 0.500 mg/ml, for 24 h. The cell survival plot showed a dose-dependent response curve (Figure 23), where the NBc treatment reduced cell proliferation from 6.66% (0.016 mg/ml) to 20.45% (0.500 mg/ml) exposure, whereas the cell proliferation of untreated cells used as a control was only 0.89% (0 mg/ml), respectively.

It was observed that cell viability slightly decreased upon increasing NBcs concentration (Figure 23). However, the NBcs concentration used for the internalization experiments was only 0.150 mg/ml, which showed a cellular viability higher than 85%. Furthermore, the cell cytotoxicity test is evaluated in 24 h, which is much longer as compared to the NBc internalization time (8 h). In this context, we could tell that the NBc would not negatively affect the cell viability in the concentration and incubation time selected for our experiments.

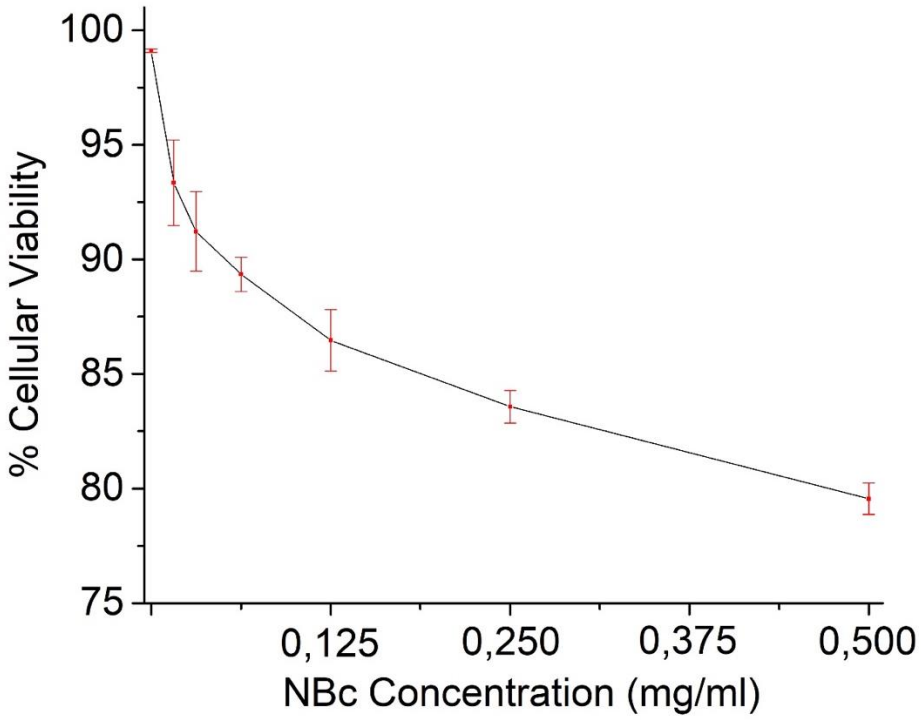

Figure 23. Cellular viability of NBc in Cardiomyocytes at 0.150 mg/ml of NBc.

5.6 Conclusions

- The affinity of the CTP-coated NPcs (NBc) for the cardiac cells was successfully demonstrated by their internalization at high extent in only 8 h, respect to the bare PNcs, tested as a control for 14 h.

- Affinity of the CTP for the cardyomyocite cellular membrane was maintained after the PNcs functionalization process, because the endocytosis process by the cardiac cell is not affected.

- The NBcs concentration used to obtain a high internalization extent in cardiomyocytes in 8 h, demonstrated to produce 85% cell viability, which strongly suggests that NBc could act, as a carrier for drug delivery systems in biomedical applications.

5.7 General conclusions, scope and perspectives

General conclusions

In this master thesis we solved the necessity expressed by Avula and co-workers (2012) of developing functional nanocarriers with specificity to cardiac cells and capacity for drug release by photo-triggering. In the same manner, the as-developed NBc demonstrated to have high specificity to cardyomiocytes, thus circumventing the necessity of an "atrial-selective" drugs, recently expressed by Ravens (2017).

From the chronological findings of this work we can conclude:

- The Cardiac Targeting Peptide was selected as the proper bioreceptor with affinity to cardiomyocytes. This is a transmembrane peptide with the capacity to be internalized by the cardiac cell, which is not lost after the functionalization of the PNcs with CTP. Such high affinity has been demonstrated by its easy internalization in the cardiomyocytes cytoplasm, through an endocytosis process.

- It was possible to functionalize the CTP at the surface of the UV-photosensitive nanocarriers, and to obtain an optimum size of the resultant nanobioconjugates, that allows for crossing the cellular membrane of the cardiomyocytes without damage. Such NBcs resulted to be biocompatible and demonstrated capacity to transport both hydrophobic drugs and photosensitizers, which are photosensitive to UV-light.

- The NBcs developed have the capacity to act as a carrier for drug photoactivated-delivery systems, thus increasing the potential of bionanotechnology in biomedical applications.

Future prospect of functional nanocarriers as possible treatment for atrial fibrillation

In this master thesis the NBc synthetized comprises the UV-photosensitive nanocarriers liked to the CTP bioreceptors. This NBcs demonstrated to be faster internalized by the cardiomyocyte cells and to have the capability to transport antiarrhythmic hydrophobic drugs, which can be in turn released by short-term UV irradiation. Future research in our

laboratory is directed to demonstrate the drug delivery inside of the cardiomyocyte cells through UV-light, by using a fluorescent drug model, as depicted in Figure 24. A further step would be to test this treatment in AF animal models to then carry out clinical trials.

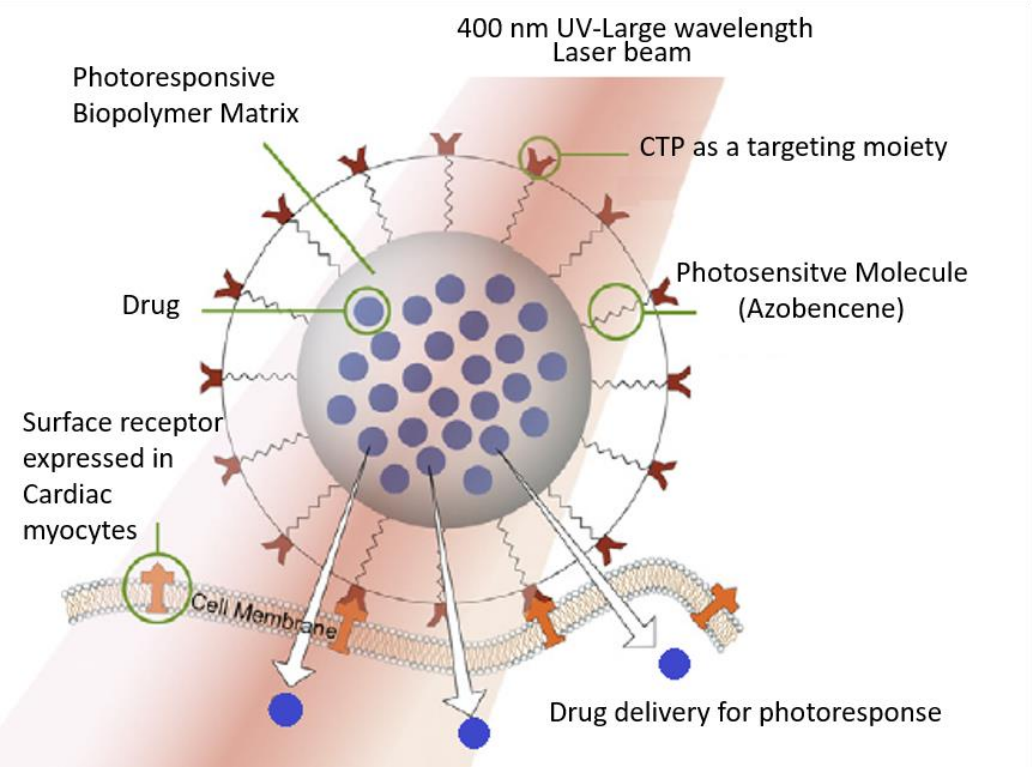

Figure 24. Future Progress of functional nanoparticles for targeted drug delivery as possible treatment for atrial fibrillation (Modified image from Avula (2012) [7].

5.8 Academic production

Presentation at International School

Pedro Alejandro Mena-Giraldo, PEPTIDE-FUNCTIONALIZED NANOPARTICLES FOR SELECTIVE PHOTODYNAMIC THERAPY IN CARDIAC CELLS. In the "*Sao Paulo School of Advanced Science on Nanophotonics and XV Jorge Andre Swieca School on Nonlinear and Quantum Optics"*, at the Gleb Wataghin Physics Institute – IFGW/UNICAMP, held in Campinas, Brazil from July 17th to 29th, 2016. Modality: Oral presentation. International scholarship.

Presentation at International Congress

Sandra Milena Perez Buitrago, Pedro Alejandro Mena Giraldo, Rodolfo Pinal, Lina Marcela Hoyos, PHOTORESPONSIVE NANOCARRIERS FOR LOCALIZED DRUG DELIVERY, in the Interfacing Nanometer and Micrometer-Scale Structures to the Bio-world Symposium at the "*XXV International Materials Research Congress"* held in Cancun, Mexico from August 14th to 19th, 2016. Modality: Oral presentation.

Scientific article published

Pedro Mena-Giraldo, Sandra Pérez-Buitrago, Rodolfo Pinal, Lina Hoyos, SÍNTESIS DE N-SUCCINIL-QUITOSANO Y FORMACIÓN DE NANOMICELAS PARA TRANSPORTE DE FÁRMACOS HIDRÓFOBOS, Revista Investigaciones Aplicadas, ISSN 2011-0413, Vol. 9, No. 2 (2015), PP. 125 – 131, Medellín – Colombia.

This article is the first stage of the nanocarriers synthesis used in the master thesis. It is index in: Publindex categoría C, ProQuest Agriculture Journals, Ebsco-Fuente académica premier - Fuente Académica Plus, MIAR, Informe académico (Gale) and Dialnet.

Scientific article in process to submit

Pedro Mena-Giraldo, Sandra Pérez-Buitrago, Maritza Londoño, Isabel Ortiz, Lina Hoyos, Jahir Orozco, PEPTIDE-FUNCTIONALIZED PHOTOSENSITIVE NANOCARRIERS BASED- N-SUCCINYL CHITOSAN FOR SPECIFIC DELIVERY OF DRUG IN CARDIOMYOCYTES. In the process of submitting.

REFERENCES

[1] Y. Xu, et al., "Atrial remodeling: New pathophysiological mechanism of atrial fibrillation," Medical Hypotheses, vol. 80, no. 1, p. 53–56, 2013.

[2] A. Avezum, et al., "How Can We Avoid a Stroke Crisis? Working Group Report: Stroke Prevention in Patients with Atrial Fibrillation," Tech. rep. August. Bayer HealthCare Pharmaceuticals, pp. 1-85, 2011.

[3] E. Bontempo and L. J. Goralnick, "Atrial Fibrillation," *Emergency medicine clinics of North America,* vol. 33, no. 3, p. 597–612, 2015.

[4] J. Camm, et al., "Guidelines for the management of atrial fibrillation: the Task Force for the Management of Atrial Fibrillation of the European Society of Cardiology (ESC)," *European heart journal,* vol. 31, no. 19, p. 2369–2429, 2010.

[5] C. T. January, et al., "AHA/ACC/HRS Guideline for the Management of Patients With Atrial Fibrillation: Executive Summary: A Report of the American College of Cardiology/American Heart Association Task Force on Practice Guidelines and the Heart Rhythm Society," *Journal of the American College of Cardiology,* vol. 212, 2014.

[6] D. P. ZIPES and J. Jalife, "Cardiac Electrophysiology: From Cell to Bedside," *Philadelphia: Elsevier,* vol. 6, p. 1043–1049, 2014.

[7] U. M. Avula, G. Kim, Y. E. K. Lee, F. Morady, R. Kopelman and J. Kalifa, (2012). Cell-specific nanoplatform-enabled photodynamic therapy for cardiac cells. Heart Rhythm, 9(9), 1504-1509.

[8] U. Avula, et al., "Left Atrium Nanoplatform-Enabled Targeted Photodynamic Ablation: Preliminary Results In Vivo," *Heart Rhythm,* vol. 10, no. 11, p. 1747, 2013.

[9] S. Pérez-Buitrago, "Phototriggerable polymer-based nanoparticles for localized delivery of dofetilide," Doctoral Thesis: in Medical Sciences, Faculty of Medicine, Universidad Pontificia Bolivariana, Medellín, 2018.

[10] U. Ravens and K. E. Odening, "Atrial fibrillation: Therapeutic potential of atrial K+ channel blockers," *Pharmacology & Therapeutics,* vol. 176, p. 13–21, 2017.

[11] M. Rawat, D. Singh and S. Saraf (2006). Nanocarriers: promising vehicle for bioactive drugs. Biological and Pharmaceutical Bulletin, 29(9), 1790-1798.

[12] A. Z. Wilczewska, K. Niemirowicz, K. H. Markiewicz and H. Car, "Nanoparticles as drug delivery systems," *Pharmacol, Reports,* vol. 64, p. 1020–1037 , 2012.

[13] Eubamiranda, "Liposomas una revision bibliografica," 17 11 2010. [Online]. Available: https://liposomas.wordpress.com/2010/11/17/formacion-de-liposomas/. [Accessed 19 12 2017].

[14] M. Rawat, D. Singh and S. Saraf (2006). Nanocarriers: promising vehicle for bioactive drugs. Biological and Pharmaceutical Bulletin, 29(9), 1790-1798.

[15] K. Letchford and H. Burt, "A review of the formation and classification of amphiphilic block copolymer nanoparticulate structures: micelles nanospheres, nanicapsules and polymersomes," *Eur. J. Pharm. Biopharm,* vol. 65, pp. 69-259, 2007.

[16] S. H. Giddi, M. Arunagirinathan and R. J. Bellare, "Self-assembled surfactant nano-structures important in drug delivery: a review," *Indian J. Exp. Biol.,* vol. 45, pp. 133-59, 2007.

[17] E. Paszko, C. Ehrhardt, M. Senge, D. Kelleher and j. Reynolds, "Nanodrug applications in photodynamic therapy," *Photodiagnosis and Photodynamic Therapy,* vol. 8, pp. 14-29, 2011.

[18] R. N. Fogoros, "Electrophysiologic Testing," *Chichester, UK: JohnWiley {&} Sons, Ltd,* 2012.

[19] A. J. Workman, G. L. Smith and A. C. Rankin, "Mechanisms of termination and prevention of atrial fibrillation by drug therapy," *Pharmacology {&} therapeutics,* vol. 131, no. 2, p. 221–241, 2011.

[20] J. Tamargo and J. López-Sendón, "Novel therapeutic targets for the treatment of heart failure," *Nat Rev Drug Discov ,* vol. 10, no. 7, p. 536–555, 2011.

[21] G. Michael, et al., "Remodelling of cardiac repolarization: How homeostatic responses can lead to arrhythmogenesis," *Cardiovascular Research ,* vol. 81, no. 3, p. 491–499, 2009.

[22] I. Savelieva, et al., "Upstream therapies for management of atrial fibrillation: review of clinical evidence and implications for European Society of Cardiology guidelines. Part I: primary prevention.," *Europace ,* vol. 13, no. 3, p. 308–328, 2011 .

[23] I. Savelieva, et al., "Upstream therapies for management of atrial fibrillation: review of clinical evidence and implications for European Society of Cardiology guidelines. Part II: secondary prevention.," *Europace ,* vol. 13, no. 5, p. 610–625, 2011.

[24] P. Kirchhof, et al., "PITX2c Is Expressed in the Adult Left Atrium, and Reducing Pitx2c Expression Promotes Atrial Fibrillation Inducibility and Complex Changes in Gene Expression," *Circulation: Cardiovascular Genetics ,* vol. 4 , no. 2, p. 123–133, 2011.

[25] J. Wang, et al., "Pitx2 prevents susceptibility to atrial arrhythmias by inhibiting left-sided pacemaker specification," *Proceedings of the National Academy of Sciences,* vol. 107, no. 21, p. 9753–9758, 2010.

[26] D. F. Gudbjartsson, et al., "Variants conferring risk of atrial fibrillation on chromosome 4q25," *Nature,* vol. 448 , no. 7151, p. 353–357, 2007.

[27] P. Alboni, et al., "Outpatient Treatment of Recent-Onset Atrial Fibrillation with the “Pill-in-the-Pocket” Approach.," *New England Journal of Medicine,* vol. 351 , no. 23, p. 2384–2391, 2004.

[28] P. Kirchhof and G. Breithardt, "New concepts for old drugs to maintain sinus rhythm in patients with atrial fibrillation," *Heart Rhythm,* vol. 4, no. 6, p. 790 –793, 2007.

[29] U. Schotten, et al., "Pathophysiological Mechanisms of Atrial Fibrillation: A Translational Appraisal," *Physiological Reviews,* vol. 91, no. 1, p. 265–325, 2011.

[30] S. M. Narayan, D. E. Krummen and W. J. Rappel, "Clinical Mapping Approach To Diagnose Electrical Rotors and Focal Impulse Sources for Human Atrial Fibrillation," *J Cardiovasc Electrophysiol ,* vol. 23 , no. 5, pp. 447-454, 2012.

[31] A. Castaño, et al., " Coronary artery pathophysiology after radiofrequency catheter ablation: review and perspectives," *Heart rhythm : the official journal of the Heart Rhythm Society,* vol. 8, no. 12, pp. 1975-1980, 2011.

[32] D. I. Vanegas, "Cual es la realidad de los tratamientos de la fibrilacion auricular en latinoamerica?," *simposio latinoamericano de fibrilacion auricular,* vol. 1, 2011.

[33] E. Ruoslahti, "Peptides as targeting elements and tissue penetration devices for nanoparticles," *Adv Mater,* vol. 24, no. 28, p. 3747–56., 2012.

[34] H. J. Hah, et al., "Methylene Blue-Conjugated Hydrogel Nanoparticles and Tumor-Cell Targeted Photodynamic Therapy," *Macromolecular Bioscience ,* vol. 11, no. 1, p. 90–99., 2011.

[35] W. Tang, et al., "Encapsulation of methylene blue in polyacrylamide nanoparticle platforms protects its photodynamic effectiveness," *Biochemical and biophysical research communications ,* vol. 369, no. 2, p. 579–583, 2008.

[36] A. Jhaveri, P. Deshpande and v. Torchilin, "Stimuli-sensitive nanopreparations for combination cancer therapy. Journal of controlled release," *official journal of the Controlled Release Society ,* vol. 190, p. 352–370, 2014.

[37] M. e. a. Zahid, "Identification of a cardiac specific protein transduction domain by in Vivo biopanning using a M13 phage peptide display library in mice," *PLoS ONE ,* vol. 5, no. 8, 2010.

[38] S. Kanki, et al., "Journal of Molecular and Cellular Cardiology Identi fi cation of targeting peptides for ischemic myocardium by in vivo phage display," *Journal of Molecular and Cellular Cardiology ,* vol. 50, no. 5, p. 841–848, 2011.

[39] S. S. K. Dasa, et al., "Development of target-specific liposomes for delivering small molecule drugs after reperfused myocardial infarction," *Journal of Controlled Release,* vol. 220, pp. 556-567, 2015.

[40] S. Lu, et al., "Targeting of embryonic stem cells by peptide-conjugated quantum dots," *PLoS ONE ,* vol. 5, no. 8, 2010.

[41] M. Liu, et al., "Heart-targeted nanoscale drug delivery systems," *Journal of Biomedical Nanotechnology,* vol. 9, no. 2038–2062, p. 10, 2014.

[42] Y. Gao, et al., "Nanotechnology-based intelligent drug design for cancer metastasis treatment," *Biotechnology Advances,* vol. 32 , no. 4, p. 761–777, 2014.

[43] T. L. Andresen, D. H. Thompson and T. Kaasgaard, "Enzyme-triggered nanomedicine: drug release strategies in cancer therapy," *Molecular membrane biology,* vol. 27, no. 7, p. 353–363, 2010.

[44] P. Rai, et al., "Development and applications of photo-triggered theranostic agents," *Advanced drug delivery reviews ,* vol. 62 , no. 11, p. 1094–1124, 2010.

[45] Y. Gao, et al., "Nanotechnology-based intelligent drug design for cancer metastasis treatment," *Biotechnology Advances,* vol. 32, no. 4, p. 761–777, 2014.

[46] R. Cheng, et al., "Dual and multi-stimuli responsive polymeric nanoparticles for programmed site-specific drug delivery.," *Biomaterials,* vol. 34 , no. 14, p. 3647–3657, 2013.

[47] Y. Li, G. H. Gao and D. S. Lee, "Stimulus-sensitive polymeric nanoparticles and their applications as drug and gene carriers," *Advanced healthcare materials,* vol. 2, no. 3, p. 388–417, 2013.

[48] M. Motornov, et al., "Stimuli-responsive nanoparticles, nanogels and capsules for integrated multifunctional intelligent systems," *Progress in Polymer Science,* vol. 35 , no. 2, p. 174–211, 2010.

[49] Y. Li, et al., "Amphiphilic azo polymer spheres, colloidal monolayers, and photoinduced chromophore orientation," *Langmuir ,* vol. 21, no. 14, p. 6567–6571, 2005.

[50] X. Wang, "Azo polymer colloidal spheres: formation, two- dimensional array, and photoresponsive properties," *Smart Light-Responsive Materials,* p. 177–213, 2009.

[51] N. Li, Y. Li and X. Wang, "Photoresponsive submicron-sized hollow spheres obtained from amphiphilic azobenzene-containing random copolymer," *Polymer ,* vol. 53 , no. 18, p. 3975–3985, 2012.

[52] I. Moleavin, et al., "Amphiphilic azopolymers capable to generate photo-sensitive micelles," *Central European Journal of Chemistry,* vol. 9, no. 6, p. 1117–1125, 2011.

[53] Y. Zhao, "Azobenzene-containing block copolymer micelles: toward light-controllable nanocarriers," *Smart Light-Responsive Materials,* p. 215–242, 2005.

[54] M. S. Kim and S. L. Diamond, "Photocleavage of o-nitrobenzyl ether derivatives for rapid biomedical release applications," *Bioorganic {&} medicinal chemistry letters ,* vol. 16, no. 15, p. 4007–4010, 2006 .

[55] M. Ito, Y. Nobuhara and K. Yamaguchi, "Fabrication of Self-Assembled Monolayers possessing Photodegradable 6-Bromo-7-hydroxycoumarinylmethyl Derivative," *Polymer Preprints,* 2012.

[56] J. Cao, et al., "Near-infrared light-triggered dissociation of block copolymer micelles for controlled drug release," *Biomaterials,* vol. 34, no. 26, pp. 6272-6283, 2013.

[57] G. Liu, et al., "An NIR-responsive and sugar-targeted polypeptide composite nanomedicine for intracellular cancer therapy," *Chemical Communications ,* vol. 50 , no. 2, p. 12538–12541, 2014.

[58] C. Bao, et al., "Long conjugated 2-nitrobenzyl derivative caged anticancer prodrugs with visible light regulated release: preparation and functionalizations," *Organic and biomolecular chemistry ,* vol. 10 , no. 27, p. 5238–5244, 2012.

[59] M. M. Cardoso, I. Peça and A. C. A. Roque, "Antibody-Conjugated Nanoparticles for Therapeutic Applications," *Current Medicinal Chemistry,* vol. 19, pp. 3103-3127, 2012,.

[60] R. L. Juliano, R. Alam, V. Dixit and H. M. Kang (2009). Cell-targeting and cell-penetrating peptides for delivery of therapeutic and imaging agents. Wiley Interdisciplinary Reviews: Nanomedicine and Nanobiotechnology, 1(3), 324-335.

[61] "PepBank," Massachusetts General Hospital, Harvard University, [Online]. Available: http://pepbank.mgh.harvard.edu/interactions/details/58328. [Accessed 18 01 2018].

[62] L. P. Kozlowski, "Protein isoelectric point calculator," Biology Direct 11:55., 2016. [Online]. Available: http://isoelectric.ovh.org/calculate.php. [Accessed 05 04 2016].

[63] D. Sehgal and I. K. Vijay, "A method for the high efficiency of water-soluble carbodiimide-mediated amidation," *Anal Biochem,* vol. 218, no. 1, pp. 87-91, 1994.

[64] Z. H. Maayah and G. Abdelhamid, "Development of cellular hypertrophy by 8-hydroxyeicosatetraenoic acid in the human ventricular cardiomyocyte , RL-14 cell line , is implicated by MAPK and NF- k B," p. 241–259, 2015.

[65] Z. H. Maayah, et al., "Human fetal ventricular cardiomyocyte , RL-14 cell line , is a promising model to study drug metabolizing enzymes and their associated arachidonic acid metabolites," *Journal of Pharmacological and Toxicological Methods,* vol. 71, pp. 33-41, 2015.

[66] "ATCC. Fetal human ventricular cardiomyocyte cell line with SV - 40 gene : RL14 (PTA - 1499)," *Tech. rep,* p. 6597, 2014.

[67] L. C. Kobashigawa, et al., "Metformin protects cardiomyocyte from doxorubicin induced cytotoxicity through an AMP-activated protein kinase dependent signaling pathway: An in Vitro study," *PLoS ONE 9,* vol. 8, 2014.

[68] K. Bilmin, B. Kopczynska and P. Grieb, "Influence of serum and albumin on the in vitro anandamide cytotoxicity toward C6 glioma cells assessed by the MTT cell viability assay: implications for the methodology of the MTT tests," *Folia Neuropathol ,* vol. 51, no. 1, pp. 44-50, 2013.

[69] S. Muela Serrano, (1999, July). Validación y aplicación de un método colorimétrico para el cribado farmacológico primario de nuevos productos de síntesis actividad tripanocida. In Anales de la Real Academia de Farmacia (Vol. 65, No. 3, pp. 599-626).

[70] I. Ortiz, "PROTOCOLO MTT," Tech. rep. Medellín: Universidad Pontificia Bolivariana, Medellín, 2014.

[71] C. Ladavière and R. Gref, (2015). Toward an optimized treatment of intracellular bacterial infections: input of nanoparticulate drug delivery systems. Nanomedicine, 10(19), 3033-3055.

[72] M. Ruiz-Villarreal, "Endocytosis types," wikimedia.org, 27 07 2007. [Online]. Available: https://commons.wikimedia.org/wiki/File:Endocytosis_types.svg. [Accessed 05 02 2018].

[73] A. Jhaveri, P. Deshpande and V. Torchilin, "Stimuli-sensitive nanopreparations for combination cancer therapy," *Journal of Controlled Release,* vol. 190, p. 352–370, 2014.

[74] M. Zahid, B. E. Phillips, S. M. Albers, N. Giannoukakis, S. C. Watkins and P. D. Robbins, (2010). Identification of a cardiac specific protein transduction domain by in vivo biopanning using a M13 phage peptide display library in mice. PloS one, 5(8), e12252.

5.9 Supplemental results

Covariance Parameter Estimates		
Cov Parm	Estimate	Standard Error
Hours*Bloque*Rep	0.01217	0.03010
Residual	0.1044	.

Type III Tests of Fixed Effects				
Effect	Num DF	Den DF	F Value	Pr > F
Hours	4	30	3488.07	<.0001
Bloque	2	30	0.00	0.9960
Hours*Bloque	8	30	0.08	0.9996

Differences of Hours Least Squares Means Adjustment for Multiple Comparisons: Tukey							
Hours	Hours	Estimate	Standard Error	DF	t Value	Pr > |t|	Adj P
5	6	-0.8286	0.1609	30	-5.15	<.0001	0.0001
5	7	-2.2813	0.1609	30	-14.17	<.0001	<.0001
5	8	-15.8977	0.1609	30	-98.78	<.0001	<.0001
5	14	-0.8142	0.1609	30	-5.06	<.0001	0.0002
6	7	-1.4527	0.1609	30	-9.03	<.0001	<.0001
6	8	-15.0691	0.1609	30	-93.63	<.0001	<.0001
6	14	0.01444	0.1609	30	0.09	0.9291	1.0000
7	8	-13.6164	0.1609	30	-84.60	<.0001	<.0001
7	14	1.4671	0.1609	30	9.12	<.0001	<.0001
8	14	15.0835	0.1609	30	93.72	<.0001	<.0001